Quantum filtering for a two-level atom driven by two counter-propagating photons

Zhiyuan Dong · **Guofeng Zhang** ·
Nina H. Amini

Abstract The purpose of this paper is to propose quantum filters for a two-level atom driven by two continuous-mode counter-propagating photons and under continuous measurements. Two scenarios of multiple measurements, 1) homodyne detection plus photodetection, and 2) two homodyne detections, are discussed. Filtering equations for both cases are derived explicitly. As demonstration, the two input photons with rising exponential and Gaussian pulse shapes are used to excite a two-level atom under two homodyne detection measurements. Simulations reveal scaling relations between atom-photon coupling and photonic pulse shape for maximum atomic excitation.

1 Introduction

Quantum filters, pioneered by Belavkin [6,7,8,9], has attracted lots of attention over the past decades [22,10,5,50]. In quantum optics, quantum filters, also known as quantum trajectories or stochastic master equations, are of great importance in measurement feedback control [50,52,23,53]. The problems of quantum filtering for systems driven by Gaussian states, including vacuum state, thermal state, coherent state, and squeezed state, have been well studied, see, e.g., [17,12,34,18]. On the other hand, as single- and multi-photon states can nowadays be generated in real experiments [39,49,51,31,29,36,32,

Zhiyuan Dong · Guofeng Zhang
Department of Applied Mathematics, The Hong Kong Polytechnic University, Hong Kong, China
E-mail: Guofeng.Zhang@polyu.edu.hk

Nina H. Amini
Laboratoire des signaux et systèmes (L2S), CNRS-CentraleSupélec-Université Paris-Sud, Université Paris-Saclay, 3, rue Joliot Curie, 91190 Gif-sur-Yvette, France

47], more and more research has been concentrated on atomic excitation [49, 4, 43, 40] and quantum filter design [28, 26, 45, 14, 20, 3] for systems driven by single or multiple photons.

Single-photon states play a fundamental role in quantum information, quantum computation, quantum measurements and control [33, 31, 32, 47]. Quantum filtering for systems driven by fields in single-photon states has been investigated in [28, 25, 26, 11, 19, 20, 21, 16], among others. Particularly, quantum filters have been used to analyze conditional phase shifts on an optical cavity in [11]. The master equations and filter equations for single-photon quantum filtering have been derived explicitly by using Markovian or non-Markovian embeddings in [28, 25, 26]. Recently, imperfect measurements and vacuum noise have also been considered in single-photon quantum filter design [14, 20, 16].

In addition to single-photon input states, the problem of quantum filtering for systems driven by multi-photon states has been discussed in [45, 27, 15]. A general multi-photon filtering framework has been proposed in [45] for both homodyne detection measurement and photon-counting measurement. Moreover, multiple measurements have been used to overcome the undesired vacuum noise and improve estimation performance [15]. In this paper, we derive quantum filters for a two-level atom driven by two counter-propagating input photons. Two cases of combined measurements have been considered, namely 1) joint homodyne and photon-counting measurements and 2) two homodyne measurements. The explicit forms of the quantum filters are given for both cases. As demonstration, the excitation probabilities have been simulated for a two-level atom which is driven by two counter-propagating photons with rising exponential and Gaussian pulse shapes, respectively. Several system parameters have been compared to achieve the optimal excitation probabilities in each scenario. For the single-photon filtering problem, it is well known that the optimal ratio for atomic excitation with a rising exponential pulse shape incident photon is $\gamma = \kappa$, where γ is the full width at half maximum (FWHM) of the photon wave packet and κ is the decay rate of the atom [46, 49, 38]. On the other hand, if the incident photon is with Gaussian pulse shape, the optimal ratio is $\Omega = 1.46\kappa$, where Ω is the photon bandwidth [46, 42, 49, 28, 4]. In this paper, when the two-level atom is driven by two counter-propagating identical photons, it is shown that the maximum of excitation probability attains at $\gamma = 5\kappa$ for rising exponential pulse shapes (see the blue curve in Fig. 5(a)), while $\Omega = 2*1.46\kappa$ for the Gaussian pulse shapes (see Fig. 6).

Many features in the few-photon-atom interaction can be observed and analyzed in a simple way, such as master equations and their variants, see, e.g. [43, 40]. On the other hand, quantum filters reveal the conditioned dynamics of the system under continuous measurements, which cannot be observed in a master equation, as the latter is the ensemble average of the former. Indeed, in section 4.2, numerical simulations have been performed for the study of a two-level atom driven by two counter-propagating photons with Gaussian pulse shapes. In each of the subfigures of Fig. 6, the fluctuating curves are individual quantum trajectories, whose average is given by the red solid curve in the top-right corner. Also, the master equation has been plotted in the black

solid curve in the top-right corner. It can be observed that in each subfigure the red solid curve and black solid curve almost coincide. This validates the fact that the master equation is the ensemble average of quantum trajectories, see Remark 3 in section 3.4. However, the quantum trajectories reveal more details of the dynamics that cannot be displayed by the master equation:

– Some trajectories in Fig. 6(a) can reach almost unity probability, which means the two-level atom is fully excited in these scenarios.
– In Fig. 6(a), the master equation (the black solid curve in the top-right corner) has the peak value at time $t = 4$. The average of the quantum trajectories, given by the red solid curve in the top-right corner, also reaches its maximum value at $t = 4$. Nevertheless, many trajectories reach their maximum values at different time instants, although not far away from their mean value $t = 4$. Indeed, this shows the stochastic nature of the atom-photon interaction.

Therefore, it is reasonable to say that a quantum filter is more powerful than a master equation, and is able to show more dynamics of an open quantum system under continuous measurements. Finally, since quantum filters describe the conditional evolution of physical systems under continuous measurements, they are essential for real-time measurement-based feedback control of quantum systems [50,1].

This paper is organized as follows. In section 2, we review some basic preliminaries such as the (S, L, H) formalism, quantum filtering, and continuous-mode single-photon states. System augmentation used in this paper is introduced in section 3.1 and the result of quantum filtering for systems driven by vacuum input states [18] is briefly recalled in section 3.2. Then filtering equations with multiple measurements for a two-level atom driven by two counter-propagating single-photons are derived explicitly. Specifically, the joint homodyne-photoncounting measurement case is discussed in section 3.3, while the joint homodyne-homodyne measurement case is discussed in section 3.4. The excitation probabilities of a two-level atom interacting with photons with rising exponential pulse shapes and Gaussian pulse shapes are numerically simulated and discussed in section 4. Section 5 concludes this paper.

Notation. Let $|\eta\rangle$ be the initial state of the two-level atom and $|0\rangle$ be the vacuum field state. Given a column vector of operators or complex numbers $X = [x_1, \cdots, x_n]^T$, the adjoint operator or complex conjugate of X is denoted by $X^\# = [x_1^*, \cdots, x_n^*]^T$, and $X^\dagger = (X^\#)^T$. The commutator between operators A and B is defined to be $[A, B] = AB - BA$. Two superoperators are

$$\text{Lindbladian} : \mathcal{L}_G X \equiv -i[X, H] + \mathcal{D}_L X,$$
$$\text{Liouvillian} : \mathcal{L}_G^\star \rho \equiv -i[H, \rho] + \mathcal{D}_L^\star \rho,$$

where $\mathcal{D}_L X = L^\dagger X L - \frac{1}{2}(L^\dagger L X + X L^\dagger L)$, and $\mathcal{D}_L^\star \rho = L \rho L^\dagger - \frac{1}{2}(L^\dagger L \rho + \rho L^\dagger L)$. Finally, δ_{jk} is the Kronecker delta function and $\delta(t - r)$ is the Dirac delta function.

2 Preliminary

2.1 Open quantum systems in the (S, L, H) formalism

In this paper, the system under study is a two-level atom that is driven by two counter-propagating photons. This is an open quantum system for which the so-called (S, L, H) formalism has proven very convenient [24, 52, 48, 44, 13]. Here, S is a scattering operator satisfying $S^\dagger S = SS^\dagger = I$, L denotes the coupling between the system and field, and the initial system Hamiltonian is described by the self-adjoint operator H.
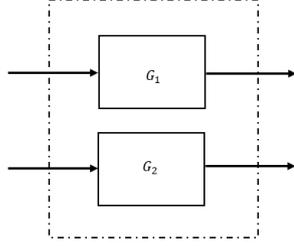
Fig. 1 Concatenation product of two quantum systems G_1 and G_2

Given two quantum systems $G_1 = (S_1, L_1, H_1)$ and $G_2 = (S_2, L_2, H_2)$, their concatenation product $G_1 \boxplus G_2$, as shown in Fig. 1, is introduced in [24]

$$G_1 \boxplus G_2 = \left(\begin{bmatrix} S_1 & 0 \\ 0 & S_2 \end{bmatrix}, \begin{bmatrix} L_1 \\ L_2 \end{bmatrix}, H_1 + H_2 \right). \tag{1}$$
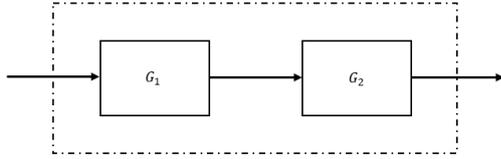
Fig. 2 Series product of two quantum systems G_1 and G_2

Moreover, if G_1 and G_2 have the same number of field channels, their series product $G_2 \lhd G_1$, as shown in Fig. 2, can be defined by

$$G_2 \lhd G_1 = \left(S_2 S_1, L_2 + S_2 L_1, H_1 + H_2 + \mathrm{Im}\{L_2^\dagger S_2 L_1\} \right). \tag{2}$$

2.2 Quantum filtering

As we study in this paper the problem of quantum filtering of a two-level atom driven by two counter-propagating photons, in this section we briefly introduce the basics of quantum filtering.

Let the annihilation operator for the j-th input field be $b_j(t)$ and its adjoint operator be $b_j^*(t)$. Since the field we consider is in continuous-mode, the following commutation relation holds:

$$[b_j(t), b_k^*(r)] = \delta_{jk}\delta(t - r), \quad j, k = 1, 2. \tag{3}$$

Denote $b(t) = \begin{bmatrix} b_1(t) \\ b_2(t) \end{bmatrix}$. The integrated annihilation, creation, and gauge processes are given by

$$B(t) = \int_{t_0}^t b(s)ds, \ B^{\#}(t) = \int_{t_0}^t b^{\#}(s)ds, \ \varLambda(t) = \int_{t_0}^t b^{\#}(s)b^T(s)ds,$$

respectively, where t_0 is the time when the system and field start interaction. Due to (3), these quantum stochastic processes satisfy

$$dB_j(t)dB_k^*(t) = \delta_{jk}dt, \quad dB_j(t)d\varLambda_{kl}(t) = \delta_{jk}dB_l(t),$$
$$d\varLambda_{jk}(t)dB_l^*(t) = \delta_{kl}dB_j^*(t), \quad d\varLambda_{jk}(t)d\varLambda_{lm}(t) = \delta_{kl}d\varLambda_{jm}(t). \tag{4}$$

The unitary operator $U(t)$ on the tensor product Hilbert spaces System $\otimes$ Field can be used to describe the dynamical evolution of a quantum system in the (S, L, H) formalism, which is the solution to the quantum stochastic differential equation (QSDE)

$$dU(t) = \left\{ -\left(iH + \frac{1}{2}L^{\dagger}L\right)dt + LdB^{\dagger}(t) - L^{\dagger}SdB(t) + \mathrm{Tr}[S - I]d\varLambda(t) \right\}U(t) \tag{5}$$

with the initial condition $U(t_0) = I$ (identity operator).

Based on (4) and (5), the time evolution of the system operator X, denoted by

$$j_t(X) \equiv X(t) = U^{\dagger}(t)(X_{\mathrm{system}} \otimes I_{\mathrm{field}})U(t), \tag{6}$$

is given by

$$dj_t(X) = j_t(\mathcal{L}_G X)dt + dB^{\dagger}(t)j_t(S^{\dagger}[X, L])$$
$$+ j_t([L^{\dagger}, X]S)dB(t) + \mathrm{Tr}[j_t(S^{\dagger}XS - X)d\varLambda(t)]. \tag{7}$$

The dynamical evolution of the output field in the input-output formalism is given by

$$dB_{\mathrm{out}}(t) = L(t)dt + S(t)dB(t),$$
$$d\varLambda_{\mathrm{out}}(t) = L^{\#}(t)L^T(t)dt + S^{\#}(t)dB^{\#}(t)L^T(t)$$
$$+ L^{\#}(t)dB^T(t)S^T(t) + S^{\#}(t)d\varLambda(t)S^T(t),$$

where $B_{\text{out}}(t) = U^\dagger(t)(I_{\text{system}} \otimes B(t))U(t)$ is the integrated output annihilation operator, and $\Lambda_{\text{out}}(t) = U^\dagger(t)(I_{\text{system}} \otimes \Lambda(t))U(t)$ is the output gauge process.

The output fields can be continuously measured, and from these measurements one can construct quantum filters to study the conditioned dynamics of the system. Homodyne detection and photon-counting measurements are commonly used in quantum optical experiments. In the case of homodyne detection, the measurement equation is

$$Y(t) = U^\dagger(t)(I_{\text{system}} \otimes (B(t) + B^\#(t)))U(t), \tag{8}$$

while in the case of photon-counting measurement

$$Y(t) = U^\dagger(t)(I_{\text{system}} \otimes \Lambda(t))U(t). \tag{9}$$

Both of them enjoy the self-non-demolition property

$$[Y(t), Y(r)] = 0, \quad t_0 \leq r \leq t, \tag{10}$$

and the non-demolition property

$$[X(t), Y(s)] = 0, \quad t_0 \leq s \leq t. \tag{11}$$

The quantum conditional expectation is defined as

$$\hat{X}(t) \equiv \pi_t(X) = \mathbb{E}[j_t(X)|\mathcal{Y}_t], \tag{12}$$

where $\mathbb{E}$ denotes the expectation and the commutative von Neumann algebra $\mathcal{Y}_t$ is generated by the past measurement observation $\{Y(s) : t_0 \leq s \leq t\}$. Simply speaking, the quantum filtering problem is to find the minimum of the least mean squares estimation $\mathbb{E}[\{\pi_t(X) - j_t(X)\}^2]$ for the system observables $j_t(X)$. The conditioned system density operator $\rho(t)$ can be obtained by means of $\pi_t(X) = \text{Tr}\{(\rho(t))^\dagger X\}$. It turns out that $\rho(t)$ is a solution to a system of stochastic differential equations, which is called *quantum filter* in the quantum control community or *quantum trajectories* in the quantum optics community, see, e.g., [6,10,5,26,45,50,13].

2.3 Continuous-mode single-photon states

Let $b^*(t)$ be the creation operator of a travelling light field. Define an integrated creation operator $B^*(\xi)$ for a single photon with pulse shape $\xi(t)$ to be

$$B^*(\xi) = \int_{-\infty}^{\infty} \xi(t)b^*(t)dt, \tag{13}$$

where $|\xi(t)|^2 dt$ is the probability of finding the photon in the time interval $[t, t + dt)$, which satisfies the normalization condition $\int_{-\infty}^{\infty} |\xi(t)|^2 dt = 1$. A continuous-mode single-photon state can be given by

$$|1_\xi\rangle = B^*(\xi)|0\rangle, \tag{14}$$
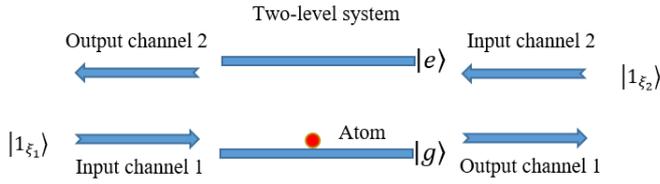
Fig. 3 A two-level atom is driven by two counter-propagating photons, one in each input channel. After interaction, the two photons are in the two output channels. Then the light fields in the two output channels are mixed by a beam splitter, the resulting light fields are measured. (The beam splitter and the measurement devices are not shown in this figure, but they can be found in Fig. 4.)

which means that the operator $B^*(\xi)$ acts on the vacuum state $|0\rangle$ to generate a single-photon state for the travelling light field. It can be verified that

$$dB(t)|1_\xi\rangle = \xi(t)dt|0\rangle, \quad d\Lambda(t)|1_\xi\rangle = \xi(t)dB^*(t)|0\rangle. \tag{15}$$

The problem of quantum filtering for systems driven continuous-mode single-photon fields has been investigated in a series of papers, e.g., [28, 25, 26, 11, 19, 20, 16].

3 Quantum Filtering with Multiple Measurements

In this section, the filtering equations for a two-level atom driven by two counter-propagating continuous-mode photons and under multiple measurements are derived explicitly, see Figs. 3-4. The main ideas of the derivation of the quantum filters are summarized as follows. As shown in Fig. 4, two ancillas, A_1 and A_2, are used to generate single-photon states $|1_{\xi_1}\rangle$ and $|1_{\xi_2}\rangle$ from the vacuum input fields 1 and 2, the mechanism of such photon generation is discussed in details in section 3.1. The two photons generated interact with the two-level atom, denoted G in Fig. 4, after interaction they are scattered into two output channels. These output channels are mixed by a beam splitter to produce two output light fields (namely Output 1 and Output 2 in Fig. 4), which in the sequel are continuously measured by homodyne detectors or photodetectors. The augmented system G_E (ancillas plus two-level atom plus beam splitter) in Fig. 4 is driven by two vacuum input fields, the filter for this augmented system is presented in section 3.2. However, as we are interested in the quantum filters for the two-level system under continuous measurements, we have to perform partial trace over the two ancillas A_1 and A_2, which is done in sections 3.3 and 3.4. More specifically, in section 3.3, the quantum filter is derived when the output fields are measured by a homodyne detector and a photodetector, while in section 3.4, the quantum filter is derived when the output fields are measured by two homodyne detectors.
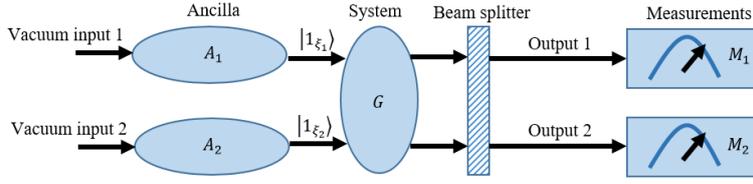
Fig. 4 Quantum system depiction: A_1, A_2 are the two ancillas which cascade the quantum system G, two measurements M_1 and M_2 will be used as the detectors, e.g., homodyne detector or photodetector. The augmented system (from the vacuum input to measurement) is denoted by G_E for later use.

3.1 System augmentation

Fig. 4 presents a more detailed quantum system depiction for the scheme shown in Fig. 3. Two quantum signal generators (ancillas A_1, A_2) are used to cascade the two-level atom G. The augmented system $G_E = \mathbf{S}_b \lhd G \lhd (A_1 \boxplus A_2)$ could be obtained by means of the concatenation and series products introduced in section 2.1. In what follows, we specify the parameter for the augmented system G_E. First, consider the beam splitter in Fig. 4, which in the (S, L, H) formalism is given by $\mathbf{S}_b = (S_b, 0, 0)$ with

$$S_b = \begin{bmatrix} \sqrt{1 - r^2} & r \\ -r & \sqrt{1 - r^2} \end{bmatrix}, \quad 0 \le r \le 1. \tag{16}$$

Next, we consider the two-level atom G. In this paper, we consider the *on-resonance* case, i.e., the carrier frequency of the single-photon light field is equal to the transition frequency between the excited and ground states of the two-level atom. As a result, the system Hamiltonian $H = 0$, which maximizes the atom-photon interaction [49,4,40]. In the (S, L, H) formalism, we have $G = (I_2, L, 0)$, where $L = \begin{bmatrix} \sqrt{\kappa_1} \\ \sqrt{\kappa_2} \end{bmatrix} \sigma_-$, where σ_- is the lowering operator of the two-level atom G. Finally, we look at the two ancillas A_1 and A_2, who in the (SL, H) formalism are given by

$$A_1 = (I, L_1, 0), \quad A_2 = (I, L_2, 0), \tag{17}$$

where the coupling operators are $L_1 = \lambda_1(t)\sigma_{-1}$ and $L_2 = \lambda_2(t)\sigma_{-2}$, respectively. Here, σ_{-1} and σ_{-2} correspond to lowering operators from the excited state $|\uparrow\rangle$ to the ground state $|\downarrow\rangle$ for the two ancillas. The rising operators will be denoted by σ_{+1} and σ_{+2} respectively. Ordinary functions $\lambda_1(t)$ and $\lambda_2(t)$ are given by

$$\lambda_1(t) = \frac{\xi_1(t)}{\sqrt{w_1(t)}}, \quad \lambda_2(t) = \frac{\xi_2(t)}{\sqrt{w_2(t)}}, \tag{18}$$

where $w_1(t) = \int_t^\infty |\xi_1(s)|^2 ds$, $w_2(t) = \int_t^\infty |\xi_2(s)|^2 ds$, and $\xi_1(t)$ and $\xi_2(t)$ are the corresponding input pulse shapes in the first and second channels. As

shown in [28, 29, 16], if the ancilla A_i $(i = 1, 2)$ is initialized in the excited state $|\uparrow\rangle$ and driven by a vacuum field, it will generate a single photon state $|1_{\xi_i}\rangle$ $(i = 1, 2)$. That is why A_1 and A_2 are called signal generators.

By the concatenation and series products introduced in section 2.1, the augmented system $G_E = \mathbf{S}_b \lhd G \lhd (A_1 \boxplus A_2)$ in Fig. 4 can be re-parameterized as

$$G_E = (S_t, L_t, H_t), \tag{19}$$

where

$$S_t = \begin{bmatrix} \sqrt{1 - r^2} & r \\ -r & \sqrt{1 - r^2} \end{bmatrix},$$

$$L_t = \begin{bmatrix} \sqrt{1 - r^2}(L_1 + \sqrt{\kappa_1}\sigma_-) + r(L_2 + \sqrt{\kappa_2}\sigma_-) \\ -r(L_1 + \sqrt{\kappa_1}\sigma_-) + \sqrt{1 - r^2}(L_2 + \sqrt{\kappa_2}\sigma_-) \end{bmatrix},$$

$$H_t = \frac{1}{2i}(\sqrt{\kappa_1}\sigma_+ L_1 + \sqrt{\kappa_2}\sigma_+ L_2 - \sqrt{\kappa_1}L_1^\dagger \sigma_- - \sqrt{\kappa_2}L_2^\dagger \sigma_-).$$

In the following, we use $\tilde{U}(t)$ to describe the evolution operator for the augmented system G_E. Then the following equality can be verified

$$\mathbb{E}_{\eta\xi}[X(t)] = \mathbb{E}_{\uparrow\eta0}[\tilde{U}^\dagger(t)(I_{\text{ancilla}} \otimes X \otimes I_{\text{field}})\tilde{U}(t)], \tag{20}$$

where on the right hand side, $\uparrow$ means that the ancillas are initialized in the excited state, η is the initial state of the two-level atom, and 0 denotes the vacuum input field state. In the next section, we present the quantum filter for the augmented system G_E.

3.2 Quantum filter for the augmented system G_E

By means of system augmentation introduced in the preceding section, the augmented system G_E is now driven by two vacuum fields, see Fig. 4. The problem of quantum filtering for this type of systems has been studied in [18]. In this section, we cite the main result of [18] in order to derive quantum filters for a two-level atom driven by two counter-propagating photons in sections 3.3 and 3.4.

As discussed in [18], a general measurement equation, which is a function of annihilation, creation and gauge processes of the output fields, may be defined as

$$dY(t) = F_1^\# dB_{\text{out}}^\#(t) + F_1 dB_{\text{out}}(t) + F_2 \text{diag}(d\Lambda_{\text{out}}(t)). \tag{21}$$

Moreover, a set of measurements $Y(t)$ is self-commutative if and only if the constant matrices F_1 and F_2 satisfy

$$\begin{bmatrix} F_1 & F_1^\# \end{bmatrix} \begin{bmatrix} \mathbf{0} & I \\ -I & \mathbf{0} \end{bmatrix} \begin{bmatrix} F_1^T \\ F_1^\dagger \end{bmatrix} = \mathbf{0},$$

$$\begin{bmatrix} F_2 & F_1^\# \end{bmatrix} \begin{bmatrix} \mathbf{0} & I \\ -I & \mathbf{0} \end{bmatrix} \begin{bmatrix} F_2^T \\ F_1^\dagger \end{bmatrix} = \mathbf{0},$$

$$\begin{bmatrix} F_2 & F_1 \end{bmatrix} \begin{bmatrix} \mathbf{0} & I \\ -I & \mathbf{0} \end{bmatrix} \begin{bmatrix} F_2^T \\ F_1^T \end{bmatrix} = \mathbf{0}.$$

In the following, we cite the main result in [18], which presents the quantum filter for an open quantum system driven by vacuum input fields.

Lemma 1 *[18, Theorem 3.2] Let $\{Y_{i,t}, i = 1, 2, \ldots, N\}$ be a set of N compatible measurement outputs for a quantum system $\mathcal{E}$, i.e., $Y_{i,t}$ satisfy the self-commutative and non-demolition properties. With* **vacuum** *input state, the quantum filter is given by*

$$d\tilde{X}_t = \pi_t[\mathcal{L}_\mathcal{E}(\tilde{X}_t)]dt + \sum_{i=1}^{N} \beta_{i,t} dW_{i,t}, \tag{22}$$

where $dW_{i,t} = dY_{i,t} - \pi_t(dY_{i,t})$ is a martingale process for each measurement output and $\beta_{i,t}$ is the corresponding gain given by

$$\zeta^T = \pi_t(\tilde{X}_t dY_t^T) - \pi_t(\tilde{X}_t)\pi_t(dY_t^T) + \pi_t\left([L_t^\dagger, \tilde{X}_t]S_t dB dY_t^T\right), \tag{23}$$

$$\Sigma = \pi_t(dY_t dY_t^T), \quad \beta = \Sigma^{-1}\zeta \tag{24}$$

with Σ being assumed to be non-singular.

The augmented system G_E discussed in section 3.1 is an open quantum system driven by vacuum input fields. As a result, Lemma 1 can be used to derive its quantum filter. However, in this paper what we are interested in are quantum filters for a two-level atom driven by two continuous-mode counter-propagating photons. Hence, more developments have to be carried out, which are tasks for sections 3.3 and 3.4.

3.3 Quantum filter for the case of joint homodyne and photon-counting measurements

In this section, we present the quantum filter for the case where the output fields are measured by a combination of homodyne detector and photodetector.

For the augmented system G_E introduced in section 3.1, if we choose $F_1 = \begin{bmatrix} 1 & 0 \\ 0 & 0 \end{bmatrix}$ and $F_2 = \begin{bmatrix} 0 & 0 \\ 0 & 1 \end{bmatrix}$ in the general measurement equation (21), then we have

$$\begin{aligned} dY_1(t) &= \sqrt{1 - r^2}\Big[dB_1(t) + dB_1^*(t) + (L_1 + \sqrt{\kappa_1}\sigma_-)dt \\ &\quad + (L_1^* + \sqrt{\kappa_1}\sigma_+)dt\Big] + r\Big[dB_2(t) + dB_2^*(t) \\ &\quad + (L_2 + \sqrt{\kappa_2}\sigma_-)dt + (L_2^* + \sqrt{\kappa_2}\sigma_+)dt\Big], \\ dY_2(t) &= \Big[r^2(L_1^* + \sqrt{\kappa_1}\sigma_+)(L_1 + \sqrt{\kappa_1}\sigma_-) \\ &\quad - r\sqrt{1 - r^2}(L_2^* + \sqrt{\kappa_2}\sigma_+)(L_1 + \sqrt{\kappa_1}\sigma_-) \\ &\quad - r\sqrt{1 - r^2}(L_1^* + \sqrt{\kappa_1}\sigma_+)(L_2 + \sqrt{\kappa_2}\sigma_-) \end{aligned} \tag{25}$$

$$+(1-r^2)(L_2^* + \sqrt{\kappa_2}\sigma_+)(L_2 + \sqrt{\kappa_2}\sigma_-)\Big]dt$$
$$+\Big[r^2(L_1^* + \sqrt{\kappa_1}\sigma_+) - r\sqrt{1-r^2}(L_2^* + \sqrt{\kappa_2}\sigma_+)\Big]dB_1(t)$$
$$+\Big[r^2(L_1 + \sqrt{\kappa_1}\sigma_-) - r\sqrt{1-r^2}(L_2 + \sqrt{\kappa_2}\sigma_-)\Big]dB_1^*(t)$$
$$+\Big[(1-r^2)(L_2^* + \sqrt{\kappa_2}\sigma_+) - r\sqrt{1-r^2}(L_1^* + \sqrt{\kappa_1}\sigma_+)\Big]dB_2(t)$$
$$+\Big[(1-r^2)(L_2 + \sqrt{\kappa_2}\sigma_-) - r\sqrt{1-r^2}(L_1 + \sqrt{\kappa_1}\sigma_-)\Big]dB_2^*(t)$$
$$+r^2 d\Lambda_{11}(t) - r\sqrt{1-r^2}d\Lambda_{21}(t) - r\sqrt{1-r^2}d\Lambda_{12}(t)$$
$$+(1-r^2)d\Lambda_{22}(t), \tag{26}$$

That is, $Y_1(t)$ is a mixture of the filed quadratures, while $Y_2(t)$ is a mixture of the filed quadratures and gauge processes.

Let $dY(t) = [dY_1(t)\ dY_2(t)]^T$. By (4), it is easy to see that

$$\tilde{\pi}_t\left[dY(t)dY^T(t)\right] = \begin{bmatrix} dt & 0 \\ 0 & \tilde{\pi}_t\left[dY_2(t)dY_2(t)\right] \end{bmatrix}, \tag{27}$$

where

$$\tilde{\pi}_t[dY_2(t)dY_2(t)] = r^2\tilde{\pi}_t\big[(L_1^\dagger + \sqrt{\kappa_1}\sigma_+)(L_1 + \sqrt{\kappa_1}\sigma_-)\big]dt$$
$$-r\sqrt{1-r^2}\tilde{\pi}_t\big[(L_1^\dagger + \sqrt{\kappa_1}\sigma_+)(L_2 + \sqrt{\kappa_2}\sigma_-)\big]dt$$
$$-r\sqrt{1-r^2}\tilde{\pi}_t\big[(L_2^\dagger + \sqrt{\kappa_2}\sigma_+)(L_1 + \sqrt{\kappa_1}\sigma_-)\big]dt$$
$$+(1-r^2)\tilde{\pi}_t\big[(L_2^\dagger + \sqrt{\kappa_2}\sigma_+)(L_2 + \sqrt{\kappa_2}\sigma_-)\big]dt.$$

The Lindblad superoperator for the augmented system in Fig. 4 can be expressed as

$$\mathcal{L}_{L_t}(A_1 \otimes A_2 \otimes X)$$
$$= \mathcal{D}_{L_1}(A_1) \otimes A_2 \otimes X + A_1 \otimes \mathcal{D}_{L_2}(A_2) \otimes X$$
$$+(\kappa_1 + \kappa_2)A_1 \otimes A_2 \otimes \mathcal{D}_{\sigma_-}(X)$$
$$+\sqrt{\kappa_1}L_1^\dagger A_1 \otimes A_2 \otimes [X, \sigma_-] + \sqrt{\kappa_1}A_1 L_1 \otimes A_2 \otimes [\sigma_+, X]$$
$$+\sqrt{\kappa_2}A_1 \otimes L_2^\dagger A_2 \otimes [X, \sigma_-] + \sqrt{\kappa_2}A_1 \otimes A_2 L_2 \otimes [\sigma_+, X]. \tag{28}$$

In what follows, let $\pi_t(X)$ be the conditional expectation of the operator X of the two-level atom G and $\tilde{\pi}_t(A_1 \otimes A_2 \otimes X)$ be the conditional expectation of the operator $A_1 \otimes A_2 \otimes X$ for the extended system G_E. Then it can be shown that

$$\pi_t^{jk;mn}(X) = \frac{\tilde{\pi}_t(Q_1^{jk} \otimes Q_2^{mn} \otimes X)}{w_1^{jk}(t)w_2^{mn}(t)}, \quad j,k,m,n = 0,1, \tag{29}$$

where Q_1^{jk}, Q_2^{mn} are the operators of ancillas A_1, A_2, which are given by

$$\begin{bmatrix} Q_i^{00} & Q_i^{01} \\ Q_i^{10} & Q_i^{11} \end{bmatrix} = \begin{bmatrix} \sigma_{+i}\sigma_{-i} & \sigma_{+i} \\ \sigma_{-i} & I \end{bmatrix}, \tag{30}$$

and

$$\begin{bmatrix} w_i^{00} & w_i^{01} \\ w_i^{10} & w_i^{11} \end{bmatrix} = \begin{bmatrix} w_i(t) & \sqrt{w_i(t)} \\ \sqrt{w_i(t)} & 1 \end{bmatrix}, \quad i = 1, 2 \tag{31}$$

with $w_i(t)$ being given in section 3.1.

Based on (29) and Lemma 1, the stochastic differential equations for the $\pi_t^{jk;mn}(X)$ can be derived. Consequently, the stochastic differential equations for the evolution of conditioned system density matrix $\rho^{jk;mn}(t)$ can be derived by means of the equivalence between the Schrödinger picture and the Heisenberg picture $\pi_t^{jk;mn}(X) = \text{Tr}\{(\rho^{jk;mn}(t))^\dagger X\}, \quad j, k, m, n = 0, 1$. The following theorem presents the filtering equation of $\rho^{jk;mn}(t)$ when the output fields are under joint homodyne detection and photon-counting measurements, as given in (25)-(26). The filtering equation for $\rho^{11;11}(t)$ is given here and the others can be found in Appendix A.

Theorem 1 *In the case of joint homodyne detection and photon-counting measurements, the quantum filter for the two-level atom G driven by two counter-propagating single-photon input states $|1_{\xi_i}\rangle$, $i = 1, 2$, is given by a system of stochastic differential equations, composed of (32) below and those in Appendix A.*

$$
\begin{aligned}
d\rho^{11;11}(t) = &\left\{ (\kappa_1 + \kappa_2)\mathcal{D}_{\sigma_-}^\star \rho^{11;11}(t) + \sqrt{\kappa_1}\xi_1(t)[\rho^{01;11}(t), \sigma_+] + \sqrt{\kappa_1}\xi_1^*(t)[\sigma_-, \rho^{10;11}(t)] \right.\\
&\left. + \sqrt{\kappa_2}\xi_2(t)[\rho^{11;01}(t), \sigma_+] + \sqrt{\kappa_2}\xi_2^*(t)[\sigma_-, \rho^{11;10}(t)] \right\}dt \\
&+ \left\{ \sqrt{1 - r^2} \left[\xi_1^*(t)\rho^{10;11}(t) + \xi_1(t)\rho^{01;11}(t) + \sqrt{\kappa_1}\rho^{11;11}(t)\sigma_+ + \sqrt{\kappa_1}\sigma_-\rho^{11;11}(t) \right] \right.\\
&\quad + r \left[\xi_2^*(t)\rho^{11;10}(t) + \xi_2(t)\rho^{11;01}(t) + \sqrt{\kappa_2}\rho^{11;11}(t)\sigma_+ + \sqrt{\kappa_2}\sigma_-\rho^{11;11}(t) \right] \\
&\quad \left. - \rho^{11;11}(t) \left[\sqrt{1 - r^2}z_{11}(t) + rz_{12}(t) \right] \right\}dW_1(t) \\
&+ \left\{ K_p^{-1}(t)\left\{ r^2 \left[2|\xi_1(t)|^2\rho^{00;11}(t) + 2\sqrt{\kappa_1}\xi_1(t)\rho^{01;11}(t)\sigma_+ + \sqrt{\kappa_1}\xi_1^*(t)\sigma_-\rho^{10;11}(t) \right.\right.\right.\\
&\quad \left. + \kappa_1\sigma_-\rho^{11;11}(t)\sigma_+ \right] - r\sqrt{1 - r^2}\left[2\xi_1^*(t)\xi_2(t)\rho^{10;01}(t) + \sqrt{\kappa_2}\xi_1^*(t)\sigma_-\rho^{10;11}(t) \right.\\
&\quad + 2\sqrt{\kappa_1}\xi_2(t)\rho^{11;01}(t)\sigma_+ + 2\xi_1(t)\xi_2^*(t)\rho^{01;10}(t) + \sqrt{\kappa_1}\xi_2^*(t)\sigma_-\rho^{11;10}(t) \\
&\quad \left. + 2\sqrt{\kappa_2}\xi_1(t)\rho^{01;11}(t)\sigma_+ \right] + (1 - r^2)\left[2|\xi_2(t)|^2\rho^{11;00}(t) + \sqrt{\kappa_2}\xi_2^*(t)\sigma_-\rho^{11;10}(t) \right.\\
&\quad \left.\left.\left. + 2\sqrt{\kappa_2}\xi_2(t)\rho^{11;01}(t)\sigma_+ + \kappa_2\sigma_-\rho^{11;11}(t)\sigma_+ \right]\right\} - \rho^{11;11}(t) \right\}dN(t),
\end{aligned}
\tag{32}
$$

where

$$\rho^{01;11}(t) = (\rho^{10;11}(t))^\dagger, \quad \rho^{11;01}(t) = (\rho^{11;10}(t))^\dagger, \tag{33}$$
$$\rho^{10;01}(t) = (\rho^{01;10}(t))^\dagger, \quad \rho^{01;01}(t) = (\rho^{10;10}(t))^\dagger, \tag{34}$$
$$\rho^{00;01}(t) = (\rho^{00;10}(t))^\dagger, \quad \rho^{01;00}(t) = (\rho^{10;00}(t))^\dagger, \tag{35}$$

with the initial conditions

$$\rho^{11;11}(t_0) = \rho^{11;00}(t_0) = \rho^{00;11}(t_0) = \rho^{00;00}(t_0) = |\eta\rangle\langle\eta|. \qquad (36)$$

The innovation processes $dW_1(t)$ and $dN(t)$ are given by

$$dW_1(t) = dY_1(t) - \left[\sqrt{1-r^2}k_{11}(t) + rk_{12}(t)\right]dt, \qquad (37)$$

$$dN(t) = dY_2(t) - K_p(t)dt, \qquad (38)$$

respectively, where

$$k_{11}(t) = \xi_1^*(t)\mathrm{Tr}[\rho^{10;11}(t)] + \xi_1(t)\mathrm{Tr}[\rho^{01;11}(t)] + \sqrt{\kappa_1}\mathrm{Tr}[(\sigma_+ + \sigma_-)\rho^{11;11}(t)],$$

$$k_{12}(t) = \xi_2^*(t)\mathrm{Tr}[\rho^{11;10}(t)] + \xi_2(t)\mathrm{Tr}[\rho^{11;01}(t)] + \sqrt{\kappa_2}\mathrm{Tr}[(\sigma_+ + \sigma_-)\rho^{11;11}(t)],$$

$$K_p(t) = r^2\mathrm{Tr}\left[(L_1^\dagger + \sqrt{\kappa_1}\sigma_+)(L_1 + \sqrt{\kappa_1}\sigma_-)\rho^{11;00}(t)\right]$$

$$-r\sqrt{1-r^2}\mathrm{Tr}\left[(L_2^\dagger + \sqrt{\kappa_2}\sigma_+)(L_1 + \sqrt{\kappa_1}\sigma_-)\rho^{10;01}(t)\right]$$

$$-r\sqrt{1-r^2}\mathrm{Tr}\left[(L_1^\dagger + \sqrt{\kappa_1}\sigma_+)(L_2 + \sqrt{\kappa_2}\sigma_-)\rho^{01;10}(t)\right]$$

$$+(1-r^2)\mathrm{Tr}\left[(L_2^\dagger + \sqrt{\kappa_2}\sigma_+)(L_2 + \sqrt{\kappa_2}\sigma_-)\rho^{00;11}(t)\right].$$

Remark 1 It can be verified that $\rho^{11;11}$ in Theorem 1 is indeed self-adjoint.

3.4 Quantum filter for the case of two homodyne detection measurements

In this section, we consider the case that the output fields are measured by two homodyne detectors, that is, we choose $F_1 = I_2$ and $F_2 = 0$ in the general measurement equation (21). In this case, the output fields in Fig. 4 are $dY_1(t)$ as already given in (25) and

$$dY_2(t) = -r\left[dB_1(t) + dB_1^\dagger(t) + (L_1 + \sqrt{\kappa_1}\sigma_-)dt\right.$$

$$\left. +(L_1^\dagger + \sqrt{\kappa_1}\sigma_+)dt\right] + \sqrt{1-r^2}\left[dB_2(t) + dB_2^\dagger(t)\right.$$

$$\left. +(L_2 + \sqrt{\kappa_2}\sigma_-)dt + (L_2^\dagger + \sqrt{\kappa_2}\sigma_+)dt\right]. \qquad (39)$$

Let $dY(t) = [dY_1(t) \ dY_2(t)]^T$. By (4), it is easy to see that

$$\tilde{\pi}_t\left[dY(t)dY^T(t)\right] = \begin{bmatrix} dt & 0 \\ 0 & dt \end{bmatrix}. \qquad (40)$$

The Lindblad superoperator in this case has the same form as that given in (28). With the notation (29), we have the following theorem which presents the filtering equations for the conditional system density matrix. Similar as in Theorem 1, here we only present the filtering equation for $\rho^{11;11}(t)$ while put the others in Appendix B.

Theorem 2 *In the case of two homodyne detection measurements, the quantum filter for the two-level system G driven by two counter-propagating single-photon input states $|1_{\xi_i}\rangle$, $i = 1, 2$, is given by a system of stochastic differential equations, composed of (41) below and those in Appendix B.*

$$
\begin{aligned}
d\rho^{11;11}(t) = &\left\{ (\kappa_1 + \kappa_2)\mathcal{D}^{\star}_{\sigma_-}\rho^{11;11}(t) + \sqrt{\kappa_1}\xi_1(t)[\rho^{01;11}(t), \sigma_+] + \sqrt{\kappa_1}\xi_1^*(t)[\sigma_-, \rho^{10;11}(t)] \right. \\
&\left. + \sqrt{\kappa_2}\xi_2(t)[\rho^{11;01}(t), \sigma_+] + \sqrt{\kappa_2}\xi_2^*(t)[\sigma_-, \rho^{11;10}(t)] \right\} dt \\
&+ \left\{ \sqrt{1-r^2}\left[\xi_1^*(t)\rho^{10;11}(t) + \xi_1(t)\rho^{01;11}(t) + \sqrt{\kappa_1}\rho^{11;11}(t)\sigma_+ + \sqrt{\kappa_1}\sigma_-\rho^{11;11}(t) \right] \right. \\
&+ r\left[\xi_2^*(t)\rho^{11;10}(t) + \xi_2(t)\rho^{11;01}(t) + \sqrt{\kappa_2}\rho^{11;11}(t)\sigma_+ + \sqrt{\kappa_2}\sigma_-\rho^{11;11}(t) \right] \\
&\left. - \rho^{11;11}(t)\left[\sqrt{1-r^2}z_{11}(t) + rz_{12}(t) \right] \right\} dW_1(t) \\
&+ \left\{ -r\left[\xi_1^*(t)\rho^{10;11}(t) + \xi_1(t)\rho^{01;11}(t) + \sqrt{\kappa_1}\rho^{11;11}(t)\sigma_+ + \sqrt{\kappa_1}\sigma_-\rho^{11;11}(t) \right] \right. \\
&+ \sqrt{1-r^2}\left[\xi_2^*(t)\rho^{11;10}(t) + \xi_2(t)\rho^{11;01}(t) + \sqrt{\kappa_2}\rho^{11;11}(t)\sigma_+ + \sqrt{\kappa_2}\sigma_-\rho^{11;11}(t) \right] \\
&\left. - \rho^{11;11}(t)\left[-rz_{11}(t) + \sqrt{1-r^2}z_{12}(t) \right] \right\} dW_2(t),
\end{aligned}
\tag{41}
$$

where

$$
\rho^{01;11}(t) = (\rho^{10;11}(t))^{\dagger}, \quad \rho^{11;01}(t) = (\rho^{11;10}(t))^{\dagger}, \tag{42}
$$
$$
\rho^{10;01}(t) = (\rho^{01;10}(t))^{\dagger}, \quad \rho^{01;01}(t) = (\rho^{10;10}(t))^{\dagger}, \tag{43}
$$
$$
\rho^{00;01}(t) = (\rho^{00;10}(t))^{\dagger}, \quad \rho^{01;00}(t) = (\rho^{10;00}(t))^{\dagger}, \tag{44}
$$

with the initial conditions

$$
\rho^{11;11}(t_0) = \rho^{11;00}(t_0) = \rho^{00;11}(t_0) = \rho^{00;00}(t_0) = |\eta\rangle\langle\eta|. \tag{45}
$$

The innovation processes $dW_1(t)$ and $dW_2(t)$ are given by

$$
dW_1(t) = dY_1(t) - \left[\sqrt{1-r^2}z_{11}(t) + rz_{12}(t) \right] dt, \tag{46}
$$
$$
dW_2(t) = dY_2(t) + \left[rz_{11}(t) - \sqrt{1-r^2}z_{12}(t) \right] dt, \tag{47}
$$

respectively, where

$$
z_{11}(t) = \xi_1^*(t)\mathrm{Tr}[\rho^{10;11}(t)] + \xi_1(t)\mathrm{Tr}[\rho^{01;11}(t)] + \sqrt{\kappa_1}\mathrm{Tr}[(\sigma_+ + \sigma_-)\rho^{11;11}(t)],
$$
$$
z_{12}(t) = \xi_2^*(t)\mathrm{Tr}[\rho^{11;10}(t)] + \xi_2(t)\mathrm{Tr}[\rho^{11;01}(t)] + \sqrt{\kappa_2}\mathrm{Tr}[(\sigma_+ + \sigma_-)\rho^{11;11}(t)].
$$

Remark 2 It can be verified that $\rho^{11;11}$ in Theorem 2 is indeed self-adjoint.

Remark 3 By partial tracing over the environment of the filtering equations in Theorems 1 and 2, the terms involving innovation processes $dW_1(t)$, $dN(t)$ and $dW_2(t)$ will vanish. As a result, the filtering equations in Theorems 1 and 2 reduce to the same set of master equations. In other words, a quantum master equation is an ensemble average of a quantum filter.

The following remark demonstrates that the scenario considered in this paper can be reduced to the case of a two-level atom driven by a single-channel single-photon state, which has been studied in [28, 25, 26, 11, 16].

Remark 4 If we set $\kappa_1 = 0$ and the beam splitter $S_b = I$ in (16), then the filtering equations in Theorem 1 will reduce to the quantum filter for a two-level system driven by a single-photon state under photon-counting measurement, cf. [28, Eq. (43)], [11, Eq. (3)]. On the other hand, if we set $\kappa_2 = 0$ and the beam splitter $S_b = I$, then the filtering equations in both Theorems 1 and 2 will reduce to quantum filters for a two-level system driven by a single-photon state under homodyne detection measurement, cf. [28, Eq. (42)], [11, Eq. (2)].

4 Simulation Results

In this section, we employ the quantum filters derived above to calculate the excitation probabilities of a two-level atom which is driven by two counter-propagating photons and under two homodyne detection measurements. Assume that the two-level atom is initially in the ground state $|g\rangle$. Two types of photon pulse shapes, namely rising exponential and Gaussian pulse shapes, are considered.
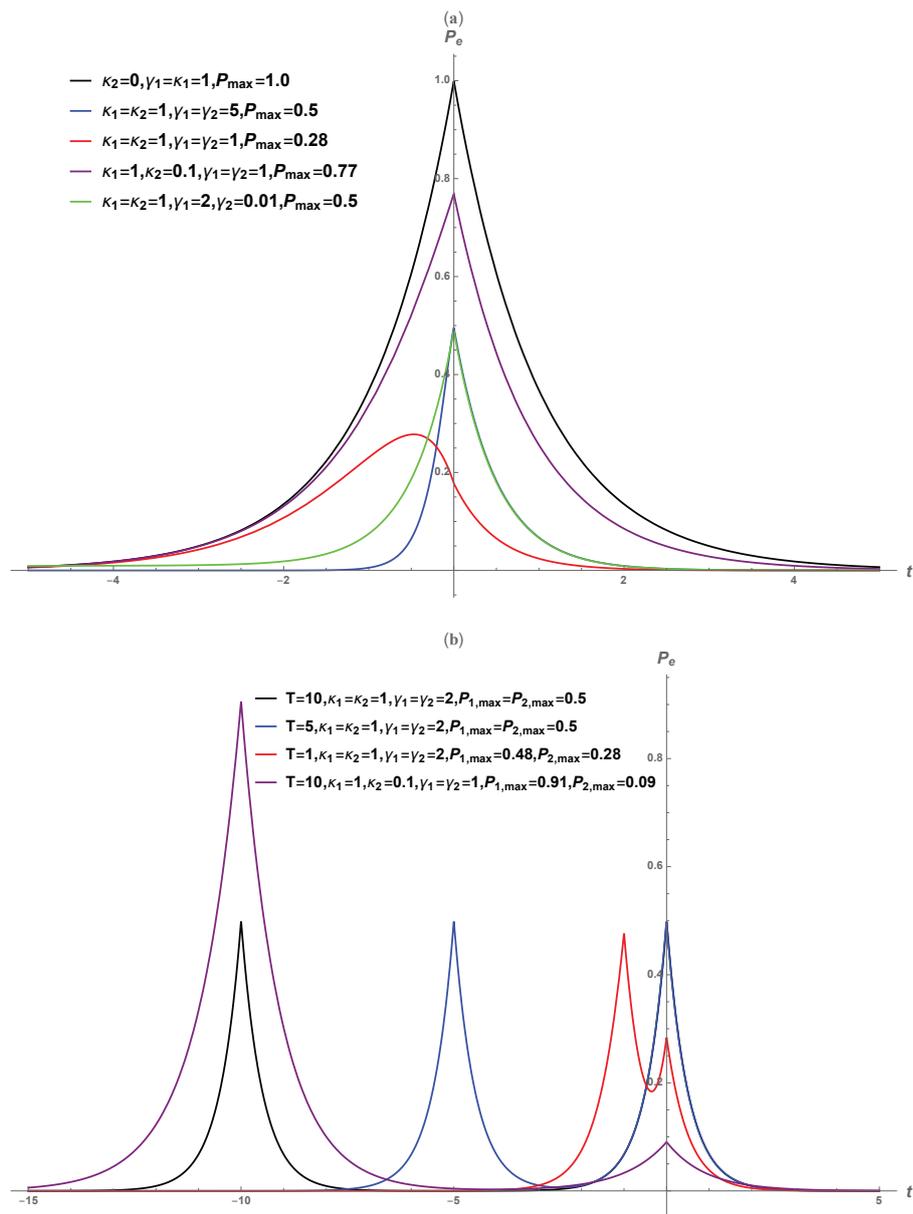
4.1 Rising exponential pulse shape

The rising exponential pulse shapes of the two photons are given by

$$\xi_i(t) = -\sqrt{\gamma_i} \; e^{\frac{\gamma_i}{2}t} H(-t), \quad i = 1, 2, \tag{48}$$

where $H(t)$ is the Heaviside function. These photons have Lorentzian lineshape functions with FWHM γ_i $(i = 1, 2)$ [2].

In this example, we use the master equation to study the excitation probabilities. As discussed in Remark 3, the master equation can be obtained by tracing out the noise terms of the quantum filter in either Theorem 1 or Theorem 2. Excitation probabilities with various pulse shape parameters are plotted in Fig. 5. We have the following observations.

(i) We look at a special case first. If we set $\kappa_2 = 0$, then, as discussed in Remark 4, we have the scenario that a two-level atom is driven by a single photon with a rising exponential pulse $\xi_1(t)$ defined in (48). Let $\gamma_1 = \kappa_1$. The excitation probability is given by the black curve in Fig. 5(a). It can be seen that the excitation probability reaches its maximum $P_{\max} = 1.0$ at time $t = 0$, after that the excited atom decays to its ground state $|g\rangle$ exponentially. This is consistent with the well-known result that a two-level atom can be fully excited by an incident photon of a rising exponential pulse shape [46, 49, 38].

Fig. 5 The excitation probabilities for a two-level atom driven by two counter-propagating photons with rising exponential pulse shapes, calculated based on the master equation.

(ii) The two-level atom is equally coupled ($\kappa_1 = \kappa_2 = \kappa$) to two identical ($\gamma_1 = \gamma_2 = \gamma$) incident photons (the blue curve in Fig. 5(a)). It is found that the excitation probability attains the maximum value $P_{\max} = 0.5$ when $\gamma = 5\kappa$. Note that in this case, the blue curve in Fig. 5(a) is not symmetric with respect to the time $t = 0$ (the part of the curve for $t > 0$ coincides with the green curve). However, if we choose $\gamma = \kappa$, then the excitation probability attains its maximum value 0.28 at $t < 0$ (the red curve in Fig. 5(a)). This reveals the complex dynamics of a two-level atom driven by two counter-propagating photons.

(iii) The two incident photons are identical but not equally coupled ($\kappa_1 \neq \kappa_2$) to the two-level atom (the purple curve in Fig. 5(a)). For instance, the coupling strength between the two-level atom and the photon in the first input channel is $\kappa_1 = 1$, while the other is $\kappa_2 = 0.1$. In this case, the interaction between the two-level atom and the photon in the second input channel is relatively weak due to the small value of κ_2. The maximum excitation probability is $P_{\max} = 0.77$ when $\gamma_1 = \gamma_2 = \kappa_1$. Obviously, this excitation probability can be close to 1 when the coupling $\kappa_2 \to 0$ as the limit is the single-photon case (the black curve in Fig. 5(a)) as discussed in item (i) above.

(iv) The two incident photons are equally coupled ($\kappa_1 = \kappa_2 = \kappa = 1$) to the two-level atom, but with different pulse shapes $\gamma_2 = 0.01$, $\gamma_1 = 2\kappa$ (the green curve in Fig. 5(a)). In this case, the incident photon in the second channel has a long temporal wave packet (small frequency bandwidth) and is reflected by the atom, see [4, Fig. 8]. Moreover, in this parameter setting, the excitation probability reaches its maximum $P_{\max} = 0.5$.

(v) The two incident photons interact with the two-level atom one after another (Fig. 5(b)). In this case, the pulse shape of the photon in the first channel is given by

$$\xi_1(t) = -\sqrt{\gamma_1} \exp(\frac{\gamma_1}{2}(t + T))H(-T - t), \qquad (49)$$

while the pulse shape of the photon in the second channel is still of the form (48). Firstly, we choose $T = 10$ (the black curve in Fig. 5(b)), that is, the two-level atom can be excited by the incident photon one after another. The excitation probability attains its maximum value $P_{\max} = 0.5$ when $\gamma = 2\kappa$. The same ratio can be found in the *simulated emission* [41, Fig. 2(a)], where the incident photon interacts with an *excited* atom. In that scenario, the probability of two photons in the second output channel P_{RR} in [41, Fig. 2(a)] attains its maximum when the pulse shape parameter is twice the coupling strength.

(vi) It can be observed that the two peak values of the excitation probability get closer as T decreases (the blue curve in Fig. 5(b)). Moreover, the excitation probability becomes smaller when the two incident photons are close to each other ($T = 1$, the red curve in Fig. 5(b)).

(vii) Lastly, we set $T = 10$, which means the two incident photons are far away from each other. The photon in the second channel is weakly coupled to

the two-level atom $\kappa_2 = 0.1$ (the purple curve in Fig. 5(b)). The excitation probability attains its maximum $P_{\max} = 0.91$ when $\gamma_1 = \kappa_1$. However, the second excitation is rather weak due to the weak coupling strength κ_2.

4.2 Gaussian pulse shape

Here, we consider the case that a two-level atom is driven by two counter-propagating photons with the Gaussian pulse shapes

$$\xi_i(t) = \left(\frac{\Omega_i^2}{2\pi} \right)^{\frac{1}{4}} \exp\left(-\frac{\Omega_i^2}{4}(t - \tau_i)^2 \right), \quad i = 1, 2, \tag{50}$$

where τ_i is the photon peak arrival time and Ω_i is the frequency bandwidth in the i-th input wave packet. If both of the output fields are measured by homodyne detectors, then quantum trajectories are those given in Theorem 2. In this scenario, the excitation probability of the two-level atom can be calculated by

$$P_e(t) = \mathrm{Tr}\left[\rho^{11;11}(t)|e\rangle\langle e| \right], \tag{51}$$

where $\rho^{11;11}(t)$ is the solution to (41).

In what follows, we study the excitation probabilities of the two-level atom by means of the master equations and quantum trajectories. In Fig. 6, the colored fluctuating curves are obtained by means of the quantum filters in Theorem 2, the black solid curves in the top-right corner are calculated by means of the master equation, and the red solid curves in the top-right corner are the results of the average of the quantum trajectories. As can be observed in all subfigures of Fig. 6 that the red curves are all very close to the black curves. This confirms the fact that a master equation is an ensemble average of a filtering equation. We have the following observations.

(i) In Fig. 6(a), we let $\kappa_2 = 0$. Then we have the single-photon quantum filtering case, See Remark 4. In this case, by the master equation, the maximum of the excitation probability is 0.8 when the optimal bandwidth $\Omega = 1.46\kappa$, see also [46, 42, 49, 28, 4]. Moreover, as can be seen in Fig. 6(a) that some individual quantum trajectories can rise up to $P_e = 1.0$, which means that the two-level atom may be fully excited. This cannot be observed by the master equation in the top-right corner of Fig. 6(a).

(ii) In Fig. 6(b), the two incident photons have different peak arrival times, $\tau_1 = 3$ and $\tau_2 = 6$. Based on the master equation it is found that the maximum value of the excitation probability is $P_e = 0.4$ when $\Omega_1 = 2 * 1.46\kappa_1$ or $\Omega_2 = 2 * 1.46\kappa_2$. That is, the two-level atom may be excited twice with the same excitation probability at time instants $t_1 = 3.5$ and $t_2 = 6.5$, respectively. Similar phenomenon can be seen in the scattering of two co-propagating input photons, where the excitation probability is even less than 0.3 [35, Fig. 5(a)]. Interestingly, the second peak value of some individual quantum trajectories can be significant larger than their first
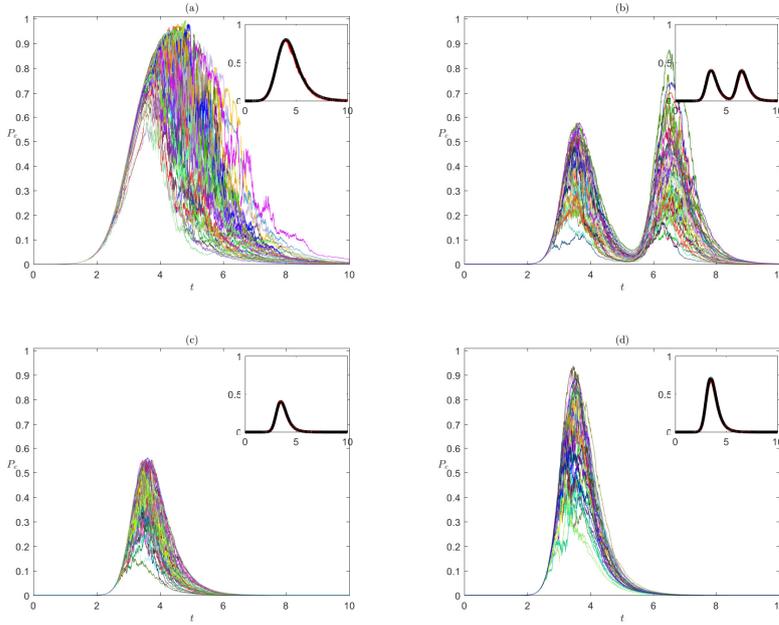
Fig. 6 Excitation probabilities of a two-level atom driven by two counter-propagating single-photon states with the Gaussian pulse shapes, calculated by the quantum master equation (the black solid curve in the top-right corner), the quantum trajectories (the fluctuating curves) and their average (the red solid curve in the top-right corner).

　　　peak value. This cannot be seen by the master equation in the top-right corner of Fig. 6(b).

(iii) In Fig. 6(c), the first channel contains a single photon of Gaussian pulse shape, while the second channel is in the vacuum state. By the master equation, the excitation probability P_e is maximized to 0.4 when $\Omega_1 = 2 * 1.46\kappa_1$. This result is consistent with the Fock-state scattering from a two-level atom [4, Fig. 7(a)], in which the maximum value of excitation probability is also 0.4 when the forward-propagating field is prepared in a Fock state with a single photon. Compared with Fig. 6(a), it can be seen that almost no quantum trajectories can rise beyond 0.6. In other words, the excitation probability becomes worse due to the vacuum input channel.

(iv) In Fig. 6(d), we choose $\tau_1 = \tau_2 = 3$, which means that the two photons interact with the two-level atom simultaneously. By the master equation, the excitation probability can attain its maximum value $P_e = 0.71$ at $t = 3.5$ when $\Omega_1 = 2 * 1.46\kappa_1$ and $\Omega_2 = 2 * 1.46\kappa_2$. This optimal bandwidth is consistent with the single-channel two-photon case studied in [45, Fig. 1], where the maximum value of the excitation probability is 0.8796 when the frequency bandwidths are $\Omega_1 = \Omega_2 = 2 * 1.46\kappa$. Moreover, there are individual quantum trajectories whose peak values are bigger than 0.9.

Remark 5 The interaction between a two-level atom and a single photon or two photons with Gaussian pulse shapes has been studied intensively in the literature. In the single-photon case, when the photon has a Gaussian pulse shape (50) with $\Omega = 1.46\kappa$, where κ is the decay rate of the two-level atom and Ω is the frequency bandwidth of the single-photon pulse shape, it is shown that the maximal excitation probability is around 0.8, see, e.g., [46], [42], [49, Fig. 1], [28, Fig. 8], [4, Fig. 2], and case (i) above. Recently, the analytical expression of the pulse shape of the output single photon has been derived in [38]. Assume the pulse shape $\xi(t)$ of the input photon is of the form (50) with photon peak arrival time $\tau = 3$ and frequency bandwidth $\Omega = 1.46\kappa$. Denote the pulse shape of the output photon by $\eta(t)$. Then it can be easily verified that $\int_{-\infty}^{4} \left(|\xi(\tau)|^2 - |\eta(\tau)|^2 \right) d\tau = 0.8$. Interestingly, the excitation probability achieves its maximum 0.8 at the time $t = 4$, see Fig. 6(a). Hence, the filtering result is consistent with the result of input-output response. The two-photon case is more complicated. Quantum filters for a two-level atom driven by a single-channel two-photon state has been derived in [45]. Numerical simulations show that the maximum value of excitation probability is 0.8796 when the frequency bandwidths $\Omega_1 = \Omega_2 = 2 * 1.46\kappa$, see [45, Fig. 1]. The analytical form of the output two-photon state has been given in [37]. Unfortunately, due to the complexity of the output two-photon state, it seems hard to exhibit the consistency between the filtering result and the input-output response result. Interestingly, as shown by the numerical simulations above, in the case that a two-level atom is driven by two counter-propagating photons with Gaussian pulse shapes, the optimal frequency bandwidths for maximal atomic excitation are $\Omega_1 = 2 * 1.46\kappa_1$ and $\Omega_2 = 2 * 1.46\kappa_2$, which is the same as the single-channel two-photon case studied in [45]. These facts indicate that the found scaling (frequency bandwidths are twice of the atomic decay rates) for maximal atomic excitation may probably have some physical meaning.

5 Conclusion

In this paper, we have investigated the problem of quantum filtering for a two-level atom driven by two counter-propagating continuous-mode photons. The explicit forms of quantum filters have been derived. We have used these quantum filters to compute the excitation probabilities when the photons are of rising exponential and Gaussian pulse shapes. Interesting scaling properties between the pulse shape and atomic decay rate have been revealed by these numerical simulations. These simulations illustrate the complex dynamics of the two-level atom driven by two counter-propagating photons, which demands for more rigorous mathematical analysis and experimental exploration.

Appendix A. In this appendix, we give the stochastic differential equations for the quantum filter mentioned in Theorem 1. (The dynamics of $\rho^{11;11}(t)$ has already been given in (32).)

$$
\begin{aligned}
d\rho^{10;11}(t) = &\left\{ (\kappa_1 + \kappa_2)\mathcal{D}^\star_{\sigma_-}\rho^{10;11}(t) + \sqrt{\kappa_1}\xi_1(t)[\rho^{00;11}(t), \sigma_+] + \sqrt{\kappa_2}\xi_2(t)[\rho^{10;01}(t), \sigma_+] \right. \\
&\left. + \sqrt{\kappa_2}\xi_2^*(t)[\sigma_-, \rho^{10;10}(t)] \right\}dt \\
&+ \left\{ \sqrt{1 - r^2}\left[\xi_1(t)\rho^{00;11}(t) + \sqrt{\kappa_1}\rho^{10;11}(t)\sigma_+ + \sqrt{\kappa_1}\sigma_-\rho^{10;11}(t) \right] \right. \\
&+ r\left[\xi_2^*(t)\rho^{10;10}(t) + \xi_2(t)\rho^{10;01}(t) + \sqrt{\kappa_2}\rho^{10;11}(t)\sigma_+ + \sqrt{\kappa_2}\sigma_-\rho^{10;11}(t) \right] \\
&\left. - \rho^{10;11}(t)\left[\sqrt{1 - r^2}z_{11}(t) + rz_{12}(t) \right] \right\}dW_1(t) \\
&+ \left\{ K_p^{-1}(t)\left\{ r^2\left[2\sqrt{\kappa_1}\xi_1(t)\rho^{00;11}(t)\sigma_+ + \kappa_1\sigma_-\rho^{10;11}(t)\sigma_+ \right] \right.\right. \\
&- r\sqrt{1 - r^2}\left[2\sqrt{\kappa_1}\xi_2(t)\rho^{10;01}(t)\sigma_+ \right. \\
&+ 2\xi_1(t)\xi_2^*(t)\rho^{00;10}(t) + \sqrt{\kappa_1}\xi_2^*(t)\sigma_+\rho^{10;10}(t) + 2\sqrt{\kappa_2}\xi_1(t)\rho^{00;11}(t)\sigma_+ \Big] \\
&+ (1 - r^2)\left[2|\xi_2(t)|^2\rho^{10;00}(t) + \sqrt{\kappa_2}\xi_2^*(t)\sigma_-\rho^{10;10}(t) + 2\sqrt{\kappa_2}\xi_2(t)\rho^{10;01}(t)\sigma_+ \right. \\
&\left.\left.\left. + \kappa_2\sigma_-\rho^{10;11}(t)\sigma_+ \right] \right\} - \rho^{10;11}(t) \right\}dN(t),
\end{aligned}
$$

$$
\begin{aligned}
d\rho^{00;11}(t) = &\left\{ (\kappa_1 + \kappa_2)\mathcal{D}^\star_{\sigma_-}\rho^{00;11}(t) + \sqrt{\kappa_2}\xi_2(t)[\rho^{00;01}(t), \sigma_+] + \sqrt{\kappa_2}\xi_2^*(t)[\sigma_-, \rho^{00;10}(t)] \right\}dt \\
&+ \left\{ \sqrt{1 - r^2}\left[\sqrt{\kappa_1}\rho^{00;11}(t)\sigma_+ + \sqrt{\kappa_1}\sigma_-\rho^{00;11}(t) \right] \right. \\
&+ r\left[\xi_2^*(t)\rho^{00;10}(t) + \xi_2(t)\rho^{00;01}(t) + \sqrt{\kappa_2}\rho^{00;11}(t)\sigma_+ + \sqrt{\kappa_2}\sigma_-\rho^{00;11}(t) \right] \\
&\left. - \rho^{00;11}(t)\left[\sqrt{1 - r^2}z_{11}(t) + rz_{12}(t) \right] \right\}dW_1(t) \\
&+ \left\{ K_p^{-1}(t)\left\{ r^2\left[\kappa_1\sigma_-\rho^{00;11}(t)\sigma_+ \right] - r\sqrt{1 - r^2}\left[2\sqrt{\kappa_1}\xi_2(t)\rho^{00;01}(t)\sigma_+ \right.\right.\right. \\
&\left. + \sqrt{\kappa_1}\xi_2^*(t)\sigma_-\rho^{00;10}(t) \right] + (1 - r^2)\left[2|\xi_2(t)|^2\rho^{00;00}(t) + \sqrt{\kappa_2}\xi_2^*(t)\sigma_-\rho^{00;10}(t) \right. \\
&\left.\left.\left. + 2\sqrt{\kappa_2}\xi_2(t)\rho^{00;01}(t)\sigma_+ + \kappa_2\sigma_-\rho^{00;11}(t)\sigma_+ \right] \right\} - \rho^{00;11}(t) \right\}dN(t),
\end{aligned}
$$

$$
\begin{aligned}
d\rho^{11;10}(t) = &\left\{ (\kappa_1 + \kappa_2)\mathcal{D}^\star_{\sigma_-}\rho^{11;10}(t) + \sqrt{\kappa_1}\xi_1(t)[\rho^{01;10}(t), \sigma_+] + \sqrt{\kappa_1}\xi_1^*(t)[\sigma_-, \rho^{10;10}(t)] \right. \\
&\left. + \sqrt{\kappa_2}\xi_2(t)[\rho^{11;00}(t), \sigma_+] \right\}dt \\
&+ \left\{ \sqrt{1 - r^2}\left[\xi_1^*(t)\rho^{10;10}(t) + \xi_1(t)\rho^{01;10}(t) + \sqrt{\kappa_1}\rho^{11;10}(t)\sigma_+ + \sqrt{\kappa_1}\sigma_-\rho^{11;10}(t) \right] \right.
\end{aligned}
$$

$$+ r \left[\xi_2(t) \rho^{11;00}(t) + \sqrt{\kappa_2} \rho^{11;10}(t) \sigma_+ + \sqrt{\kappa_2} \sigma_- \rho^{11;10}(t) \right]$$

$$- \rho^{11;10}(t) \left[\sqrt{1-r^2} z_{11}(t) + r z_{12}(t) \right] \Bigg\} dW_1(t)$$

$$+ \Bigg\{ K_p^{-1}(t) \Bigg\{ r^2 \left[2|\xi_1(t)|^2 \rho^{00;10}(t) + \sqrt{\kappa_1} \xi_1^*(t) \sigma_- \rho^{10;10}(t) + 2\sqrt{\kappa_1} \xi_1(t) \rho^{01;10}(t) \sigma_+ \right. $$

$$+ \kappa_1 \sigma_- \rho^{11;10}(t) \sigma_+ \Bigg]$$

$$- r\sqrt{1-r^2} \left[2\xi_1^*(t) \xi_2(t) \rho^{10;00}(t) + \sqrt{\kappa_2} \xi_1^*(t) \sigma_- \rho^{10;10}(t) + 2\sqrt{\kappa_1} \xi_2(t) \rho^{11;00}(t) \sigma_+ \right.$$

$$+ 2\sqrt{\kappa_2} \xi_1(t) \rho^{01;10}(t) \sigma_+ \Bigg] + (1-r^2) \left[2\sqrt{\kappa_2} \xi_2(t) \rho^{11;00}(t) \sigma_+ + \kappa_2 \sigma_- \rho^{11;10}(t) \sigma_+ \right] \Bigg\}$$

$$- \rho^{11;10}(t) \Bigg\} dN(t),$$

$$d\rho^{10;10}(t) = \Bigg\{ (\kappa_1 + \kappa_2) \mathcal{D}_{\sigma_-}^\star \rho^{10;10}(t) + \sqrt{\kappa_1} \xi_1(t) [\rho^{00;10}(t), \sigma_+] + \sqrt{\kappa_2} \xi_2(t) [\rho^{10;00}(t), \sigma_+] \Bigg\} dt$$

$$+ \Bigg\{ \sqrt{1-r^2} \left[\xi_1(t) \rho^{00;10}(t) + \sqrt{\kappa_1} \rho^{10;10}(t) \sigma_+ + \sqrt{\kappa_1} \sigma_- \rho^{10;10}(t) \right]$$

$$+ r \left[\xi_2(t) \rho^{10;00}(t) + \sqrt{\kappa_2} \rho^{10;10}(t) \sigma_+ + \sqrt{\kappa_2} \sigma_- \rho^{10;10}(t) \right]$$

$$- \rho^{10;10}(t) \left[\sqrt{1-r^2} z_{11}(t) + r z_{12}(t) \right] \Bigg\} dW_1(t)$$

$$+ \Bigg\{ K_p^{-1}(t) \Bigg\{ r^2 \left[2\sqrt{\kappa_1} \xi_1(t) \rho^{00;10}(t) \sigma_+ + \kappa_1 \sigma_- \rho^{10;10}(t) \sigma_+ \right]$$

$$- r\sqrt{1-r^2} \left[2\sqrt{\kappa_1} \xi_2(t) \rho^{10;00}(t) \sigma_+ + 2\sqrt{\kappa_2} \xi_1(t) \rho^{00;10}(t) \sigma_+ \right]$$

$$+ (1-r^2) \left[2\sqrt{\kappa_2} \xi_2(t) \rho^{10;00}(t) \sigma_+ + \kappa_2 \sigma_- \rho^{10;10}(t) \sigma_+ \right] \Bigg\} - \rho^{10;10}(t) \Bigg\} dN(t),$$

$$d\rho^{01;10}(t) = \Bigg\{ (\kappa_1 + \kappa_2) \mathcal{D}_{\sigma_-}^\star \rho^{01;10}(t) + \sqrt{\kappa_1} \xi_1^*(t) [\sigma_-, \rho^{00;10}(t)] + \sqrt{\kappa_2} \xi_2(t) [\rho^{01;00}(t), \sigma_+] \Bigg\} dt$$

$$+ \Bigg\{ \sqrt{1-r^2} \left[\xi_1^*(t) \rho^{00;10}(t) + \sqrt{\kappa_1} \rho^{01;10}(t) \sigma_+ + \sqrt{\kappa_1} \sigma_- \rho^{01;10}(t) \right]$$

$$+ r \left[\xi_2(t) \rho^{01;00}(t) + \sqrt{\kappa_2} \rho^{01;10}(t) \sigma_+ + \sqrt{\kappa_2} \sigma_- \rho^{01;10}(t) \right]$$

$$- \rho^{01;10}(t) \left[\sqrt{1-r^2} z_{11}(t) + r z_{12}(t) \right] \Bigg\} dW_1(t)$$

$$+ \Bigg\{ K_p^{-1}(t) \Bigg\{ r^2 \left[\sqrt{\kappa_1} \xi_1^*(t) \sigma_- \rho^{00;10}(t) + \kappa_1 \sigma_- \rho^{01;10}(t) \sigma_+ \right]$$

$$- r\sqrt{1-r^2} \left[2\xi_1^*(t) \xi_2(t) \rho^{00;00}(t) + \sqrt{\kappa_2} \xi_1^*(t) \sigma_- \rho^{00;10}(t) + 2\sqrt{\kappa_1} \xi_2(t) \rho^{01;00}(t) \sigma_+ \right]$$

$$+ (1-r^2) \left[2\sqrt{\kappa_2} \xi_2(t) \rho^{01;00}(t) \sigma_+ + \kappa_2 \sigma_- \rho^{01;10}(t) \sigma_+ \right] \Bigg\} - \rho^{01;10}(t) \Bigg\} dN(t),$$

$$d\rho^{00;10}(t) = \Bigg\{ (\kappa_1 + \kappa_2) \mathcal{D}_{\sigma_-}^\star \rho^{00;10}(t) + \sqrt{\kappa_2} \xi_2(t) [\rho^{00;00}(t), \sigma_+] \Bigg\} dt$$

$$+ \left\{ \sqrt{1-r^2} \left[\sqrt{\kappa_1} \rho^{00;10}(t)\sigma_+ + \sqrt{\kappa_1}\sigma_- \rho^{00;10}(t) \right] + r\left[\xi_2(t)\rho^{00;00}(t) \right. \right.$$

$$\left. + \sqrt{\kappa_2}\rho^{00;10}(t)\sigma_+ + \sqrt{\kappa_2}\sigma_- \rho^{00;10}(t) \right] - \rho^{00;10}(t)\left[\sqrt{1-r^2}z_{11}(t) + rz_{12}(t) \right] \right\} dW_1(t)$$

$$+ \left\{ K_p^{-1}(t)\left\{ r^2\left[\kappa_1\sigma_- \rho^{00;10}(t)\sigma_+ \right] - r\sqrt{1-r^2}\left[2\sqrt{\kappa_1}\xi_2(t)\rho^{00;00}(t)\sigma_+ \right] \right. \right.$$

$$\left. \left. + (1-r^2)\left[2\sqrt{\kappa_2}\xi_2(t)\rho^{00;00}(t)\sigma_+ + \kappa_2\sigma_- \rho^{00;10}(t)\sigma_+ \right] \right\} - \rho^{00;10}(t) \right\} dN(t),$$

$$d\rho^{11;00}(t) = \left\{ (\kappa_1+\kappa_2)\mathcal{D}_{\sigma_-}^\star \rho^{11;00}(t) + \sqrt{\kappa_1}\xi_1(t)[\rho^{01;00}(t), \sigma_+] + \sqrt{\kappa_1}\xi_1^*(t)[\sigma_-, \rho^{10;00}(t)] \right\} dt$$

$$+ \left\{ \sqrt{1-r^2}\left[\xi_1^*(t)\rho^{10;00}(t) + \xi_1(t)\rho^{01;00}(t) + \sqrt{\kappa_1}\rho^{11;00}(t)\sigma_+ + \sqrt{\kappa_1}\sigma_- \rho^{11;00}(t) \right] \right.$$

$$\left. + r\left[\sqrt{\kappa_2}\rho^{11;00}(t)\sigma_+ + \sqrt{\kappa_2}\sigma_- \rho^{11;00}(t) \right] - \rho^{11;00}(t)\left[\sqrt{1-r^2}z_{11}(t) + rz_{12}(t) \right] \right\} dW_1(t)$$

$$+ \left\{ K_p^{-1}(t)\left\{ r^2\left[2|\xi_1(t)|^2\rho^{00;00}(t) + \sqrt{\kappa_1}\xi_1^*(t)\sigma_- \rho^{10;00}(t) \right. \right. \right.$$

$$\left. + 2\sqrt{\kappa_1}\xi_1(t)\rho^{01;00}(t)\sigma_+ + \kappa_1\sigma_- \rho^{11;00}(t)\sigma_+ \right]$$

$$- r\sqrt{1-r^2}\left[\sqrt{\kappa_2}\xi_1^*(t)\sigma_- \rho^{10;00}(t) + 2\sqrt{\kappa_2}\xi_1(t)\rho^{01;00}(t)\sigma_+ \right]$$

$$\left. \left. + (1-r^2)\left[\kappa_2\sigma_- \rho^{11;00}(t)\sigma_+ \right] \right\} - \rho^{11;00}(t) \right\} dN(t),$$

$$d\rho^{10;00}(t) = \left\{ (\kappa_1+\kappa_2)\mathcal{D}_{\sigma_-}^\star \rho^{10;00}(t) + \sqrt{\kappa_1}\xi_1(t)[\rho^{00;00}(t), \sigma_+] \right\} dt$$

$$+ \left\{ \sqrt{1-r^2}\left[\xi_1(t)\rho^{00;00}(t) + \sqrt{\kappa_1}\rho^{10;00}(t)\sigma_+ + \sqrt{\kappa_1}\sigma_- \rho^{10;00}(t) \right] \right.$$

$$+ r\left[\sqrt{\kappa_2}\rho^{10;00}(t)\sigma_+ + \sqrt{\kappa_2}\sigma_- \rho^{10;00}(t) \right]$$

$$\left. - \rho^{10;00}(t)\left[\sqrt{1-r^2}z_{11}(t) + rz_{12}(t) \right] \right\} dW_1(t)$$

$$+ \left\{ K_p^{-1}(t)\left\{ r^2\left[2\sqrt{\kappa_1}\xi_1(t)\rho^{00;00}(t)\sigma_+ + \kappa_1\sigma_- \rho^{10;00}(t)\sigma_+ \right] \right. \right.$$

$$- r\sqrt{1-r^2}\left[2\sqrt{\kappa_2}\xi_1(t)\rho^{00;00}(t)\sigma_+ \right]$$

$$\left. \left. + (1-r^2)\left[\kappa_2\sigma_- \rho^{10;00}(t)\sigma_+ \right] \right\} - \rho^{10;00}(t) \right\} dN(t),$$

$$d\rho^{00;00}(t) = \left\{ (\kappa_1+\kappa_2)\mathcal{D}_{\sigma_-}^\star \rho^{00;00}(t) \right\} dt$$

$$+ \left\{ \sqrt{1-r^2}\left[\sqrt{\kappa_1}\rho^{00;00}(t)\sigma_+ + \sqrt{\kappa_1}\sigma_- \rho^{00;00}(t) \right] + r\left[\sqrt{\kappa_2}\rho^{00;00}(t)\sigma_+ \right. \right.$$

$$\left. \left. + \sqrt{\kappa_2}\sigma_- \rho^{00;00}(t) \right] - \rho^{00;00}(t)\left[\sqrt{1-r^2}z_{11}(t) + rz_{12}(t) \right] \right\} dW_1(t)$$

$$+\left\{K_p^{-1}(t)\left\{r^2\left[\kappa_1\sigma_-\rho^{00;00}(t)\sigma_+\right]+(1-r^2)\left[\kappa_2\sigma_-\rho^{00;00}(t)\sigma_+\right]\right\}\right.$$

$$\left.-\rho^{00;00}(t)\right\}dN(t).$$

Appendix B. In this appendix, we give the stochastic differential equations for the quantum filter mentioned in Theorem 2. (The dynamics of $\rho^{11;11}(t)$ has already been given in (41).)

$$d\rho^{10;11}(t) = \left\{(\kappa_1+\kappa_2)\mathcal{D}^\star_{\sigma_-}\rho^{10;11}(t)+\sqrt{\kappa_1}\xi_1(t)[\rho^{00;11}(t),\sigma_+]+\sqrt{\kappa_2}\xi_2(t)[\rho^{10;01}(t),\sigma_+]\right.$$

$$\left.+\sqrt{\kappa_2}\xi_2^*(t)[\sigma_-,\rho^{10;10}(t)]\right\}dt$$

$$+\left\{\sqrt{1-r^2}\left[\xi_1(t)\rho^{00;11}(t)+\sqrt{\kappa_1}\rho^{10;11}(t)\sigma_++\sqrt{\kappa_1}\sigma_-\rho^{10;11}(t)\right]\right.$$

$$+r\left[\xi_2^*(t)\rho^{10;10}(t)+\xi_2(t)\rho^{10;01}(t)+\sqrt{\kappa_2}\rho^{10;11}(t)\sigma_++\sqrt{\kappa_2}\sigma_-\rho^{10;11}(t)\right]$$

$$\left.-\rho^{10;11}(t)\left[\sqrt{1-r^2}z_{11}(t)+rz_{12}(t)\right]\right\}dW_1(t)$$

$$+\left\{-r\left[\xi_1(t)\rho^{00;11}(t)+\sqrt{\kappa_1}\rho^{10;11}(t)\sigma_++\sqrt{\kappa_1}\sigma_-\rho^{10;11}(t)\right]\right.$$

$$+\sqrt{1-r^2}\left[\xi_2^*(t)\rho^{10;10}(t)+\xi_2(t)\rho^{10;01}(t)+\sqrt{\kappa_2}\rho^{10;11}(t)\sigma_++\sqrt{\kappa_2}\sigma_-\rho^{10;11}(t)\right]$$

$$\left.-\rho^{10;11}(t)\left[-rz_{11}(t)+\sqrt{1-r^2}z_{12}(t)\right]\right\}dW_2(t),$$

$$d\rho^{00;11}(t) = \left\{(\kappa_1+\kappa_2)\mathcal{D}^\star_{\sigma_-}\rho^{00;11}(t)+\sqrt{\kappa_2}\xi_2(t)[\rho^{00;01}(t),\sigma_+]+\sqrt{\kappa_2}\xi_2^*(t)[\sigma_-,\rho^{00;10}(t)]\right\}dt$$

$$+\left\{\sqrt{1-r^2}\left[\sqrt{\kappa_1}\rho^{00;11}(t)\sigma_++\sqrt{\kappa_1}\sigma_-\rho^{00;11}(t)\right]\right.$$

$$+r\left[\xi_2^*(t)\rho^{00;10}(t)+\xi_2(t)\rho^{00;01}(t)+\sqrt{\kappa_2}\rho^{00;11}(t)\sigma_++\sqrt{\kappa_2}\sigma_-\rho^{00;11}(t)\right]$$

$$\left.-\rho^{00;11}(t)\left[\sqrt{1-r^2}z_{11}(t)+rz_{12}(t)\right]\right\}dW_1(t)$$

$$+\left\{-r\left[\sqrt{\kappa_1}\rho^{00;11}(t)\sigma_++\sqrt{\kappa_1}\sigma_-\rho^{00;11}(t)\right]\right.$$

$$+\sqrt{1-r^2}\left[\xi_2^*(t)\rho^{00;10}(t)+\xi_2(t)\rho^{00;01}(t)+\sqrt{\kappa_2}\rho^{00;11}(t)\sigma_++\sqrt{\kappa_2}\sigma_-\rho^{00;11}(t)\right]$$

$$\left.-\rho^{00;11}(t)\left[-rz_{11}(t)+\sqrt{1-r^2}z_{12}(t)\right]\right\}dW_2(t),$$

$$d\rho^{11;10}(t) = \left\{(\kappa_1+\kappa_2)\mathcal{D}^\star_{\sigma_-}\rho^{11;10}(t)+\sqrt{\kappa_1}\xi_1(t)[\rho^{01;10}(t),\sigma_+]+\sqrt{\kappa_1}\xi_1^*(t)[\sigma_-,\rho^{10;10}(t)]\right.$$

$$\left.+\sqrt{\kappa_2}\xi_2(t)[\rho^{11;00}(t),\sigma_+]\right\}dt$$

$$+\left\{\sqrt{1-r^2}\left[\xi_1^*(t)\rho^{10;10}(t)+\xi_1(t)\rho^{01;10}(t)+\sqrt{\kappa_1}\rho^{11;10}(t)\sigma_++\sqrt{\kappa_1}\sigma_-\rho^{11;10}(t)\right]\right.$$

$$+r\left[\xi_2(t)\rho^{11;00}(t)+\sqrt{\kappa_2}\rho^{11;10}(t)\sigma_++\sqrt{\kappa_2}\sigma_-\rho^{11;10}(t)\right]$$

$$- \rho^{11;10}(t) \left[\sqrt{1-r^2} z_{11}(t) + r z_{12}(t) \right] \Bigg\} dW_1(t)$$

$$+ \Bigg\{ - r \left[\xi_1^*(t) \rho^{10;10}(t) + \xi_1(t) \rho^{01;10}(t) + \sqrt{\kappa_1} \rho^{11;10}(t) \sigma_+ + \sqrt{\kappa_1} \sigma_- \rho^{11;10}(t) \right]$$

$$+ \sqrt{1-r^2} \left[\xi_2(t) \rho^{11;00}(t) + \sqrt{\kappa_2} \rho^{11;10}(t) \sigma_+ + \sqrt{\kappa_2} \sigma_- \rho^{11;10}(t) \right]$$

$$- \rho^{11;10}(t) \left[-r z_{11}(t) + \sqrt{1-r^2} z_{12}(t) \right] \Bigg\} dW_2(t),$$

$$d\rho^{10;10}(t) = \Bigg\{ (\kappa_1 + \kappa_2) \mathcal{D}_{\sigma_-}^\star \rho^{10;10}(t) + \sqrt{\kappa_1} \xi_1(t) [\rho^{00;10}(t), \sigma_+] + \sqrt{\kappa_2} \xi_2(t) [\rho^{10;00}(t), \sigma_+] \Bigg\} dt$$

$$+ \Bigg\{ \sqrt{1-r^2} \left[\xi_1(t) \rho^{00;10}(t) + \sqrt{\kappa_1} \rho^{10;10}(t) \sigma_+ + \sqrt{\kappa_1} \sigma_- \rho^{10;10}(t) \right]$$

$$+ r \left[\xi_2(t) \rho^{10;00}(t) + \sqrt{\kappa_2} \rho^{10;10}(t) \sigma_+ + \sqrt{\kappa_2} \sigma_- \rho^{10;10}(t) \right]$$

$$- \rho^{10;10}(t) \left[\sqrt{1-r^2} z_{11}(t) + r z_{12}(t) \right] \Bigg\} dW_1(t)$$

$$+ \Bigg\{ - r \left[\xi_1(t) \rho^{00;10}(t) + \sqrt{\kappa_1} \rho^{10;10}(t) \sigma_+ + \sqrt{\kappa_1} \sigma_- \rho^{10;10}(t) \right]$$

$$+ \sqrt{1-r^2} \left[\xi_2(t) \rho^{10;00}(t) + \sqrt{\kappa_2} \rho^{10;10}(t) \sigma_+ + \sqrt{\kappa_2} \sigma_- \rho^{10;10}(t) \right]$$

$$- \rho^{10;10}(t) \left[-r z_{11}(t) + \sqrt{1-r^2} z_{12}(t) \right] \Bigg\} dW_2(t),$$

$$d\rho^{01;10}(t) = \Bigg\{ (\kappa_1 + \kappa_2) \mathcal{D}_{\sigma_-}^\star \rho^{01;10}(t) + \sqrt{\kappa_1} \xi_1^*(t) [\sigma_-, \rho^{00;10}(t)] + \sqrt{\kappa_2} \xi_2(t) [\rho^{01;00}(t), \sigma_+] \Bigg\} dt$$

$$+ \Bigg\{ \sqrt{1-r^2} \left[\xi_1^*(t) \rho^{00;10}(t) + \sqrt{\kappa_1} \rho^{01;10}(t) \sigma_+ + \sqrt{\kappa_1} \sigma_- \rho^{01;10}(t) \right]$$

$$+ r \left[\xi_2(t) \rho^{01;00}(t) + \sqrt{\kappa_2} \rho^{01;10}(t) \sigma_+ + \sqrt{\kappa_2} \sigma_- \rho^{01;10}(t) \right]$$

$$- \rho^{01;10}(t) \left[\sqrt{1-r^2} z_{11}(t) + r z_{12}(t) \right] \Bigg\} dW_1(t)$$

$$+ \Bigg\{ - r \left[\xi_1^*(t) \rho^{00;10}(t) + \sqrt{\kappa_1} \rho^{01;10}(t) \sigma_+ + \sqrt{\kappa_1} \sigma_- \rho^{01;10}(t) \right]$$

$$+ \sqrt{1-r^2} \left[\xi_2(t) \rho^{01;00}(t) + \sqrt{\kappa_2} \rho^{01;10}(t) \sigma_+ + \sqrt{\kappa_2} \sigma_- \rho^{01;10}(t) \right]$$

$$- \rho^{01;10}(t) \left[-r z_{11}(t) + \sqrt{1-r^2} z_{12}(t) \right] \Bigg\} dW_2(t),$$

$$d\rho^{00;10}(t) = \Bigg\{ (\kappa_1 + \kappa_2) \mathcal{D}_{\sigma_-}^\star \rho^{00;10}(t) + \sqrt{\kappa_2} \xi_2(t) [\rho^{00;00}(t), \sigma_+] \Bigg\} dt$$

$$+ \Bigg\{ \sqrt{1-r^2} \left[\sqrt{\kappa_1} \rho^{00;10}(t) \sigma_+ + \sqrt{\kappa_1} \sigma_- \rho^{00;10}(t) \right] + r \Big[\xi_2(t) \rho^{00;00}(t)$$

$$+ \sqrt{\kappa_2} \rho^{00;10}(t) \sigma_+ + \sqrt{\kappa_2} \sigma_- \rho^{00;10}(t) \Big] - \rho^{00;10}(t) \left[\sqrt{1-r^2} z_{11}(t) + r z_{12}(t) \right] \Bigg\} dW_1(t)$$

$$+ \Bigg\{ - r \left[\sqrt{\kappa_1} \rho^{00;10}(t) \sigma_+ + \sqrt{\kappa_1} \sigma_- \rho^{00;10}(t) \right] + \sqrt{1-r^2} \Big[\xi_2(t) \rho^{00;00}(t)$$

$$+ \sqrt{\kappa_2} \rho^{00;10}(t) \sigma_+ + \sqrt{\kappa_2} \sigma_- \rho^{00;10}(t) \Big] - \rho^{00;10}(t) \left[-r z_{11}(t) + \sqrt{1-r^2} z_{12}(t) \right] \Bigg\} dW_2(t),$$

$$d\rho^{11;00}(t) = \Bigg\{ (\kappa_1 + \kappa_2) \mathcal{D}_{\sigma_-}^\star \rho^{11;00}(t) + \sqrt{\kappa_1} \xi_1(t) [\rho^{01;00}(t), \sigma_+] + \sqrt{\kappa_1} \xi_1^*(t) [\sigma_-, \rho^{10;00}(t)] \Bigg\} dt$$

$$+\left\{\sqrt{1-r^2}\left[\xi_1^*(t)\rho^{10;00}(t)+\xi_1(t)\rho^{01;00}(t)+\sqrt{\kappa_1}\rho^{11;00}(t)\sigma_++\sqrt{\kappa_1}\sigma_-\rho^{11;00}(t)\right]\right.$$

$$+r\left[\sqrt{\kappa_2}\rho^{11;00}(t)\sigma_++\sqrt{\kappa_2}\sigma_-\rho^{11;00}(t)\right]-\rho^{11;00}(t)\left[\sqrt{1-r^2}z_{11}(t)+rz_{12}(t)\right]\left.\right\}dW_1(t)$$

$$+\left\{-r\left[\xi_1^*(t)\rho^{10;00}(t)+\xi_1(t)\rho^{01;00}(t)+\sqrt{\kappa_1}\rho^{11;00}(t)\sigma_++\sqrt{\kappa_1}\sigma_-\rho^{11;00}(t)\right]\right.$$

$$+\sqrt{1-r^2}\left[\sqrt{\kappa_2}\rho^{11;00}(t)\sigma_++\sqrt{\kappa_2}\sigma_-\rho^{11;00}(t)\right]$$

$$-\rho^{11;00}(t)\left[-rz_{11}(t)+\sqrt{1-r^2}z_{12}(t)\right]\left.\right\}dW_2(t),$$

$$d\rho^{10;00}(t)=\left\{(\kappa_1+\kappa_2)\mathcal{D}_{\sigma_-}^{\star}\rho^{10;00}(t)+\sqrt{\kappa_1}\xi_1(t)[\rho^{00;00}(t),\sigma_+]\right\}dt$$

$$+\left\{\sqrt{1-r^2}\left[\xi_1(t)\rho^{00;00}(t)+\sqrt{\kappa_1}\rho^{10;00}(t)\sigma_++\sqrt{\kappa_1}\sigma_-\rho^{10;00}(t)\right]\right.$$

$$+r\left[\sqrt{\kappa_2}\rho^{10;00}(t)\sigma_++\sqrt{\kappa_2}\sigma_-\rho^{10;00}(t)\right]$$

$$-\rho^{10;00}(t)\left[\sqrt{1-r^2}z_{11}(t)+rz_{12}(t)\right]\left.\right\}dW_1(t)$$

$$+\left\{-r\left[\xi_1(t)\rho^{00;00}(t)+\sqrt{\kappa_1}\rho^{10;00}(t)\sigma_++\sqrt{\kappa_1}\sigma_-\rho^{10;00}(t)\right]\right.$$

$$+\sqrt{1-r^2}\left[\sqrt{\kappa_2}\rho^{10;00}(t)\sigma_++\sqrt{\kappa_2}\sigma_-\rho^{10;00}(t)\right]$$

$$-\rho^{10;00}(t)\left[-rz_{11}(t)+\sqrt{1-r^2}z_{12}(t)\right]\left.\right\}dW_2(t),$$

$$d\rho^{00;00}(t)=\left\{(\kappa_1+\kappa_2)\mathcal{D}_{\sigma_-}^{\star}\rho^{00;00}(t)\right\}dt$$

$$+\left\{\sqrt{1-r^2}\left[\sqrt{\kappa_1}\rho^{00;00}(t)\sigma_++\sqrt{\kappa_1}\sigma_-\rho^{00;00}(t)\right]+r\left[\sqrt{\kappa_2}\rho^{00;00}(t)\sigma_+\right.\right.$$

$$+\sqrt{\kappa_2}\sigma_-\rho^{00;00}(t)\left]-\rho^{00;00}(t)\left[\sqrt{1-r^2}z_{11}(t)+rz_{12}(t)\right]\right.\left.\right\}dW_1(t)$$

$$+\left\{-r\left[\sqrt{\kappa_1}\rho^{00;00}(t)\sigma_++\sqrt{\kappa_1}\sigma_-\rho^{00;00}(t)\right]+\sqrt{1-r^2}\left[\sqrt{\kappa_2}\rho^{00;00}(t)\sigma_+\right.\right.$$

$$+\sqrt{\kappa_2}\sigma_-\rho^{00;00}(t)\left]-\rho^{00;00}(t)\left[-rz_{11}(t)+\sqrt{1-r^2}z_{12}(t)\right]\right.\left.\right\}dW_2(t).$$

References

1. Amini, H., Somaraju, R.A., Dotsenko, I., Sayrin, C., Mirrahimi, M., Rouchon, P.: Nondemolition measurements, feedback stabilization of discrete-time quantum systems subject to non-demolition measurements with imperfections and delays. Automatica **49**(9), 2683–2692 (2013)
2. Bachor, H.A., Ralph, T.C.: A guide to experiments in quantum optics. Wiley (2004)
3. Baragiola, B.Q., Combes, J.: Quantum trajectories for propagating fock states. Phys. Rev. A **96**, 023819 (2017)
4. Baragiola, B.Q., Cook, R.L., Brańczyk, A.M., Combes, J.: N-photon wave packets interacting with an arbitrary quantum system. Phys. Rev. A **86**(1), 013811 (2012)
5. Barchielli, A., Gregoratti, M.: Quantum trajectories and measurements in continuous time: the diffusive case. Springer (2009)

6. Belavkin, V.P.: Nondemolition measurements, nonlinear filtering and dynamic programming of quantum stochastic processes. Modeling and Control of Systems 245–265 (1989)
7. Belavkin, V.P.: Quantum stochastic calculus and quantum nonlinear filtering. J. Multivariate Anal. **42**(2), 171–201 (1992)
8. Belavkin, V.P.: Quantum filtering of markov signals with white quantum noise. Quantum Communications and Measurement 381–391 (1995)
9. Belavkin, V.P.: Quantum quasi-markov processes in eventum mechanics dynamics, observation, filtering and control. Quantum Inf. Process. **12**, 1539–1626 (2013)
10. Bouten, L., Handel, R.V., James, M.R.: An introduction to quantum filtering. SIAM J. Control Optim. **46**(6), 2199–2241 (2007)
11. Carvalho, A.R.R., Hush, M.R., James, M.R.: Cavity driven by a single photon: Conditional dynamics and nonlinear phase shift. Phys. Rev. A **86**(2), 023806 (2012)
12. Chia, A., Wiseman, H.M.: Quantum theory of multiple-input–multiple-output markovian feedback with diffusive measurements. Phys. Rev. A **84**(1), 012120 (2011)
13. Combes, J., Kerckhoff, J., Sarovar, M.: The SLH framework for modeling quantum input-output networks. Advances in Physics: X **2**(3), 784–888 (2017)
14. Dong, Z., Zhang, G., Amini, H.: Quantum filtering for multiple measurements driven by fields in single-photon states. American Control Conference (ACC) 4754–4759 (2016)
15. Dong, Z., Zhang, G., Amini, H.: Quantum filtering for multiple measurements driven by two single-photon states. 12th World Congress on Intelligent Control and Automation (WCICA) 3011–3015 (2016)
16. Dong, Z., Zhang, G., Amini, H.: Single-photon quantum filtering with multiple measurements. Int. J. Adapt. Control Signal Process. **32**(3), 528–546 (2018)
17. Dum, R., Parkins, A.S., Zoller, P., Gardiner, C.W.: Monte carlo simulation of master equations in quantum optics for vacuum, thermal, and squeezed reservoirs. Phys. Rev. A **46**(7), 4382 (1992)
18. Emzir, M.F., Woolley, M.J., Petersen, I.R.: Quantum filtering for multiple diffusive and poissonian measurements. J. Phys. A: Math. Theor. **48**(38), 385302 (2015)
19. Gao, Q., Dong, D., Petersen, I.R.: Fault tolerant quantum filtering and fault detection for quantum systems. Automatica **71**, 125–134 (2016)
20. Gao, Q., Dong, D., Petersen, I.R., Rabitz, H.: Fault tolerant filtering and fault detection for quantum systems driven by fields in single photon states. J. Math. Phys. **57**(6), 062201 (2016)
21. Gao, Q., Zhang, G., Petersen, I.R.: An Exponential Quantum Projection Filter for Open Quantum Systems. Automatica **99**, 59–68, (2019)
22. Gardiner, C.W., Zoller, P.: Quantum noise. Springer Science & Business Media (2004)
23. Gough, J.E., Belavkin, V.P.: Quantum control and information processing. Quantum Inf. Process. **12**, 1397–1415 (2013)
24. Gough, J.E., James, M.R.: The series product and its application to quantum feedforward and feedback networks. IEEE Trans. Automat. Contr. **54**(11), 2530–2544 (2009)
25. Gough, J.E., James, M.R., Nurdin, H.I.: Single photon quantum filtering using non-markovian embeddings. Phil. Trans. R. Soc. A **370**(1979), 5408–5421 (2012)
26. Gough, J.E., James, M.R., Nurdin, H.I.: Quantum filtering for systems driven by fields in single photon states and superposition of coherent states using non-markovian embeddings. Quantum Inf. Process. **12**(3), 1469 (2013)
27. Gough, J.E., James, M.R., Nurdin, H.I.: Quantum trajectories for a class of continuous matrix product input states. New J. Phys. **16**(7), 075008 (2014)
28. Gough, J.E., James, M.R., Nurdin, H.I., Combes, J.: Quantum filtering for systems driven by fields in single-photon states or superposition of coherent states. Phys. Rev. A **86**(4), 043819 (2012)
29. Gough, J.E., Zhang, G.: Generating nonclassical quantum input field states with modulating filters. EPJ Quantum Technol., **2**(1), 15 (2015)
30. Hong, C.K., Ou, Z.Y., Mandel, L.: Measurement of subpicosecond time intervals between two photons by interference. Phys. Rev. Lett. **59**(18), 2044 (1987)
31. Lodahl, P., Mahmoodian, S., Stobbe, S.: Interfacing single photons and single quantum dots with photonic nanostructures. Rev. Mod. Phys. **87**(2), 347 (2015)
32. Lodahl, P., Mahmoodian, S., Stobbe, S., Rauschenbeutel, A., Schneeweiss, P., Volz, J., Pichler, H., Zoller, P.: Chiral quantum optics. Nature **541**(7638), 473 (2017)

33. Loudon, R.: The quantum theory of light. Oxford University Press (2000)
34. Nurdin, H.I.: Quantum filtering for multiple input multiple output systems driven by arbitrary zero-mean jointly gaussian input fields. Russ. J. Math. Phys. **21**(3), 386–398 (2014)
35. Nysteen, A., Kristensen, P.T., McCutcheon, D.P., Kaer, P., Mørk, J.: Scattering of two photons on a quantum emitter in a one-dimensional waveguide: exact dynamics and induced correlations. New J. Phys. **17**(2), 023030 (2015)
36. Ogawa, H., Ohdan, H., Miyata, K., Taguchi, M., Makino, K., Yonezawa, H., Yoshikawa, J.i., Furusawa, A.: Real-time quadrature measurement of a single-photon wave packet with continuous temporal-mode matching. Phys. Rev. Lett. **116**, 233602 (2016)
37. Pan, Y., Dong, D., Zhang, G.: Exact analysis of the response of quantum systems to two-photons using a QSDE approach. New J. Phys. **18**(3), 033004 (2016)
38. Pan, Y., Zhang, G., James, M.R.: Analysis and control of quantum finite-level systems driven by single-photon input states. Automatica **69**, 18–23 (2016)
39. Raymer, M.G., Noh, J., Banaszek, K., Walmsley, I.A.: Pure-state single-photon wave-packet generation by parametric down-conversion in a distributed microcavity. Phys. Rev. A **72**(2), 023825 (2005)
40. Rag, H.S. and Gea-Banacloche, J.: Two-level-atom excitation probability for single- and N-photon wave packets. Phys. Rev. A **96**(3), 033817 (2017)
41. Rephaeli, E., Fan, S.: Stimulated emission from a single excited atom in a waveguide. Phys. Rev. Lett. **108**, 143602 (2012)
42. Rephaeli, E., Shen, J.T., Fan, S.: Full inversion of a two-level atom with a single-photon pulse in one-dimensional geometries. Phys. Rev. A **82**, 033804 (2010)
43. Roulet, A., Scarani, V.: Solving the scattering of N photons on a two-level atom without computation. New J. Phys. **18**(9), 093035 (2016)
44. Sarma, G., Hamerly, R., Tezak, N., Pavlichin, D.S., Mabuchi, H.: Transformation of quantum photonic circuit models by term rewriting. IEEE Photonics J. **5**(1), 7500111-7500111 (2013)
45. Song, H., Zhang, G., Xi, Z.: Continuous-mode multi-photon filtering. SIAM J. Control Optim. **54**(3), 1602–1632 (2016)
46. Stobinska, M., Alber, G., Leuchs, G.: Perfect excitation of a matter qubit by a single photon in free space. EPL (Europhysics Letters) **86**(1), 14007 (2009)
47. Sun, S., Kim, H., Luo, Z., Solomon, G.S., Waks, E.: A single-photon switch and transistor enabled by a solid-state quantum memory. Science **361**(6397), 57–60 (2018)
48. Tezak, N., Niederberger, A., Pavlichin, D.S., Sarma, G., Mabuchi, H.: Specification of photonic circuits using quantum hardware description language. Phil. Trans. R. Soc. A **370**(1979), 5270–5290 (2012)
49. Wang, Y., Minář, J., Sheridan, L., Scarani, V.: Efficient excitation of a two-level atom by a single photon in a propagating mode. Phys. Rev. A **83**(6), 063842 (2011)
50. Wiseman, H.M., Milburn, G.J.: Quantum measurement and control. Cambridge University Press (2009)
51. Yukawa, M., Miyata, K., Mizuta, T., Yonezawa, H., Marek, P., Filip, R., Furusawa, A.: Generating superposition of up-to three photons for continuous variable quantum information processing. Opt. Express **21**(5), 5529–5535 (2013)
52. Zhang, G., James, M.R.: Quantum feedback networks and control: a brief survey. Chinese Sci. Bull. **57**(18), 2200–2214 (2012)
53. Zhang, J., Liu, Y., Wu, R., Jacobs, K., Nori, F.: Quantum feedback: Theory, experiments, and applications. Phys. Rep. **679**, 1–60 (2017)